mRNA synthesis has also been shown to be related with apoptosis induction (Stray and Air 2001).

Recently, it was reported that endoplasmic reticulum (ER) stress signaling is triggered and/or regulated by viruses (He 2006). The accumulation of unfolded proteins in the lumen of ER induces a coordinated adaptive program called unfolded protein response (UPR). UPR increases expression of molecular chaperones such as Grp94 and Grp78/BiP to facilitate proper protein folding. Recent studies showed that a variety of viral proteins trigger BiP expression during virus infection, although the effect of upregulation of BiP on virus replication is not fully understood (Jordan and others 2002; Limjindaporn and others 2009). Upon ER stress, activated inositol-requiring enzyme 1 (IRE1) initiates an unconventional splicing of *XBP1* mRNA precursor to excise its unusual intron. The spliced *XBP1* mRNA is efficiently translated into an active basic leucine zipper transcription factor to upregulate transcription of UPR genes (He 2006). Despite of UPR, unfolded proteins often accumulate and can cause apoptosis. C/EBP homologous protein (CHOP), one of the UPR downstream effectors, is a dominant-negative type inhibitor of CCAAT/enhancer-binding proteins. CHOP-mediated apoptosis is known to be coupled with a pathway that suppresses expression of Bcl-2 and intracellular glutathione and the increase of free radicals. The exact downstream target(s) of CHOP remains unclarified (He 2006). It is proposed that IRE1 plays a role in ER stress-mediated apoptosis by the interaction with tumor necrosis factor receptor-associated factor-2, which is thought to be required for the activation of procaspase-12. Activated caspase-12 cleaves procaspase-9 to generate active caspase-9, and consequently leads to activation of the caspase cascade (Urano and others 2000; Rao and others 2002a).

After influenza virus infection, BiP interacts with newly synthesized viral hemagglutinin (HA) and NA proteins (Hurtley and others 1989; Hogue and Nayak 1992). Folding and oligomerization of both proteins are normally efficient, but misfolded HA and NA are generated spontaneously in infected cells, and associate with BiP and then retain in ER. BiP-associated misfolded HA is not transported to the plasma membrane but sustained as complexes in ER for a long period before degradation. These accumulated viral proteins make BiP released from PERK, ATF6, and IRE1, which subsequently activate UPR.

In this study, we have shown that antiviral protein MxA enhances ER stress-mediated cell death after influenza virus infection. Previously, we reported that MxA accelerates cell death induced by influenza viral infection (Mibayashi and others 2002; Numajiri and others 2006). MxA promotes both caspase-dependent and caspase-independent cell death. However, the detailed stimulatory mechanism of cell death induced by MxA is unclear. We found that MxA can enhance transcription of UPR target genes. Furthermore, we have shown that MxA functionally interacts with ER chaperone BiP to promote UPR and apoptosis. Taken altogether, we propose that the cell death promotion activity of MxA plays a role for its antiviral activity.

Materials and Methods

Cells, virus infection, and transfection

Swiss mouse 3T3 cell lines, Swiss3T3-Neo and Swiss3T3-MxA cells (Staeheli and others 1986), were kindly provided by Drs. Haller and Kochs and maintained in Dulbecco's modified Eagle's medium supplemented with 10% fetal bovine serum (FBS). HeLa cells were maintained in minimal essential medium supplemented with 10% FBS. All cells were maintained at 37°C in a 5% CO_2 incubator. For infection, monolayer cultures of Swiss3T3-Neo and Swiss3T3-MxA cells in 100-mm-diameter dishes were washed twice with serum-free medium, and then infected with influenza A/PR/8 virus at a multiplicity of infection (MOI) of 10 plaque forming unit (PFU) per cell. After virus adsorption at 37°C for 1 h, the cells were washed with serum free medium and then incubated with the fresh medium at 37°C for indicated periods. Transfection of HeLa and HEK293T cells with plasmids was carried out by the standard calcium phosphate method or using transfection reagent TransIT (Mirus).

Chemical compounds

Tunicamycin (TM) and salubrinal (Sal) were purchased from Calbiochem. Brefeldin A (BFA) was purchased from Wako. These compounds were dissolved in dimethlysulfoxide.

Construction of plasmid vectors

An eukaryotic expression vector, pCHA-MxA, was constructed previously (Mibayashi and others 2002). To construct pCHA-MxA mutant vectors, pCHA-MxAΔC241 and pCHA-MxAΔC574, the insert cDNAs were amplified by polymerase chain reaction (PCR), digested with *Mlu*I and *Afl*II, and subloned into *Mlu*I- and *Afl*II-digested pCHA vector. PCR amplification was performed using pCHA-MxA as template and primers as follows: 5′-GGACGCGTATGGTTGTTTCCGAA GTGGAC-3′ for pCHA-MxAΔC241 and pCHA-MxAΔC574, 5′-GGCTTAAGTCATTAGACCACCACCAGGCTGAT-3′ for pCHA-MxAΔC241, and 5′-GGCTTAAGTCATTAGGAAGA GTCTGTTGCCGA-3′ for pCHA-MxAΔC574. Plasmids of pCHA-MxAΔC and pCHA-MxAΔN were prepared as described previously (Numajiri and others 2006).

Plasmid vectors for luciferase assays, pGL3-GRP78P(-132)-luc (Yoshida and others 1998) and p5xATF6GL3 (Wang and others 2000) designated ER stress response element (ERSE) and UPR element (UPRE) reporters, respectively, were kind gifts from Drs. Mori and Prywes, respectively. For construction of mammalian expression vector for mouse BiP, a cDNA fragments corresponding to BiP ORF with a FLAG tag at its N-terminus was amplified by reverse transcriptase (RT)-PCR with primers 5′ GCGGATCCCCGCCACCATG ACTACAAGGATGACGACAAGATGATGAAGTTCACTG TGGTGGC 3′ and 5′ GCGGATCCCTACAACTCATCTTT TTCTGATGTATC 3′ and mouse total RNA as template. PCR product was digested with *Bam*HI (TOYOBO), and inserted into the *Bam*HI site of pcDNA3 (Invitrogen) to create pcDNA3-FLAG-BiP. The details for the generation of the plasmid for hNAP-1 (Okuwaki and others 2010) will be described elsewhere.

Reverse transcriptase–polymerase chain reaction

Total RNA was isolated from Swiss3T3-Neo and Swiss3T3-MxA cells by the guanidine method. cDNA was synthesized from total RNA (0.5–2 μg) using Superscript II reverse transcriptase (RT; Invitrogen) and oligo-dT_{20} primer. PCR was performed using the above cDNAs (1/20, vol/vol) as template and a set of specific primers by pre-determined

PCR cycles, under which PCR products are semi-logarithmically amplified. Primer sequences used in this study were as follows: for mouse (m) *BiP*, 5′ AAGGTCTATGAAGGTG AACGACCCC 3′ and 5′ GACCCCAAGACATGTGAGCA ACTGC 3′; for m*XBP1*, 5′ CACGCTTGGGAATGGACACG 3′ and 5′ GATGAGGTCCCCACTGACAG 3′; for m*CHOP*, 5′ GCACGCGTATGGCAGCTGAGTCCCTGC 3′ and 5′ GCG ATATCATGCTTGGTGCAGGCTGA 3′; and for m*β-actin*, 5′ ATGGGTCAGAAGGACTCCTATGTGGG 3′ and 5′ CTAG AAGCACTTGCGGTGCACGATG 3′. The PCR products were separated on 1% agarose gel electrophoresis for *BiP*, *CHOP*, and *β-actin*, and 8% polyacrylamide gel electrophoresis (PAGE) for *XBP1*, and observed by staining with EtBr.

Real-time RT-PCR

Total RNA extraction was performed with RNeasy minikit (Qiagen), and reverse-transcribed into cDNAs by using a ReverTra Ace and oligo(dT) primer (TOYOBO). The amounts of cDNAs for *CHOP* and *β-actin* were quantified using Fast Start SYBR Green Master (Roche).

Trypan blue dye exclusion assay

Typan blue dye exclusion assays were carried out as previously described (Numajiri and others 2006). Swiss3T3-Neo and Swiss3T3-MxA cells in 60-mm-diameter dishes were treated with TM (SIGMA). After cell death induction for indicated periods, both adherent and floating cells were collected together by centrifugation. The cells were resuspend in 0.02% trypan blue (SIGMA) in phosphate-buffered saline (PBS), and dead and living cells were counted using hemocytometer.

Fluorescence-activated cell sorter analysis

Cells were treated as indicated in figure legends, collected, and then stained with propidium iodide (5 μg/mL). Fluorescence-activated cell sorting (FACS) analysis was performed using FACSCalibur instrument (BD biosciences) using CellQuest software.

Luciferase assay

The luciferase activity was determined using commercially available reagents (Promega) according to the manufacturer's protocol. The relative luciferase activity was measured for 10 s with a luminometer. The *Firefly* luciferase activity was normalized as that relative to the *Renilla* luciferase activity derived from a co-transfected control plasmid pRL-SV40 (Promega).

Indirect immunofluorescence assay

The double immunostaining of HA-MxA, FLAG-BiP, and PB1 was carried out at room temperature as follows: HeLa cells grown on glass coverslips in culture dishes were transfected with plasmid DNAs. After 24 h post transfection, the cells were infected with influenza A/PR/8 virus at MOI of 10 PFU per cell according to the protocol described above. After 8 h postinfection (hpi), cells were washed, fixed with PBS containing 4% paraformaldehyde, and then permeabilized with PBS containing 0.5% Triton X-100. The coverslips were soaked in TBS-T [25 mM Tris-HCl (pH 7.9), 137 mM NaCl, and 3 mM KCl, 0.1% Tween 20] containing 5% skim milk for 30 min. Cells were then incubated for 1 h with primary antibodies: mouse anti-HA clone 12CA5 (1:250; Roche), rat anti-HA clone 3F10 (1:3,000; Roche), rabbit anti-PB1 antibodies (1:500) (Naito and others 2007), or mouse anti-FLAG M2 (1:3,000; SIGMA) monoclonal antibodies. After washing with PBS containing 0.1% NP-40, the cells were incubated for 30 min with secondary antibodies: Alexa Fluor 488 goat anti-mouse (1:2,000; Molecular Probe, A11029), Alexa Fluor 568 goat anti-rabbit (1:2,000; Molecular Probe, A11011), and Alexa Fluor 633 goat anti-rat (1:2,000; Molecular Probe, A21094) antibodies. Coverslips were washed with PBS containing 0.1% NP-40, and incubated for 10 min with 10 mM 4′,6′-diamido-2-phenylindole dihydrochloride. After washing with PBS containing 0.1% NP-40, the coverslips were mounted on slide glasses. The cells were then observed under a fluorescence microscope (Carl Zeiss).

Immunoprecipitation assays

Transfected cells were washed with PBS and collected by centrifugation. Cells were re-suspended in IP buffer [20 mM Tris-HCl (pH 7.9), 150 mM NaCl, 30 mM KCl, 1 mM EDTA, and 0.1% NP-40]. After sonication, homogenates were centrifuged at 10,000 rpm at 4°C for 10 min. The supernatant was recovered and used for immunoprecipitation assays. Cell extracts were mixed with mouse anti-MxA KM1124 (Kyowa Medex) or mouse anti-FLAG M2 (SIGMA) antibodies and incubated at 4°C for 2 h. Immunocomplexes were recovered by the addition of protein A Sepharose Fast Flow beads (GE Healthcare). The beads were washed 3 times with IP buffer. Immunoprecipitated proteins were separated by sodium dodecyl sulfate–10% PAGE and subjected to western blot analyses using anti-HA clone 3F10 and anti-FLAG M2 antibodies.

Results

ER stress-mediated cell death is promoted by MxA

Previously, we reported that MxA has the cell death promotion activity (Mibayashi and others 2002; Numajiri and others 2006). After influenza virus infection, cells expressing MxA died faster than MxA-negative cells. Here, we have addressed how the cell death, after influenza virus infection, is triggered in cells expressing MxA. It is well established that one of the triggers of the cell death upon viral infection is the ER stress-induced cell death mechanism (He 2006). Indeed, *BiP* mRNA accumulates after influenza virus infection (Maruoka and others 2003). Thus, we first examined the expression level of *BiP* mRNA in cells expressing MxA upon influenza virus infection. In this study, we used Swiss3T3-MxA, a previously established cell line expressing MxA constitutively (Staeheli and others 1986), because MxA is IFN-inducible in certain cells and the addition of IFN may affect other IFN-related cell death/survival pathways. The level of *BiP* mRNA was upregulated in cells expressing MxA at 3 hpi (Fig. 1A). In addition, splicing of *XBP1* mRNA, an event closely correlated with ER stress, was also enhanced in cells expressing MxA at 3 hpi. These results showed that MxA enhances ER-mediated stress signaling after influenza virus infection.

Next, we examined whether MxA enhances ER stress-mediated stress signaling leading to cell death promotion upon stimuli other than influenza virus infection, because

influenza virus infection may induce a variety of cellular signaling pathways. We utilized an ER stress inducer, TM, which inhibits N-linked glycosylation and thereby causes protein accumulation in ER. Swiss3T3-MxA and Swiss3T3-Neo cells negative in MxA expression were treated with 0.5 μg/mL of TM, and then subjected to trypan blue dye exclusion assays. While TM induces cell death in both MxA-positive and control cells, the number of dead cells was 8–10 times greater in MxA-positive cells (Fig. 1B). More than 70% of MxA-positive cells died at 48 h after TM treatment.

In parallel, we examined whether caspase-12 activation is further enhanced by MxA. Caspase-12 is activated specifically in cells suffered from ER stress (Morishima and others 2002) and functions as the initiator caspase in response to a toxic insult to ER, such as treatment with TM or calcium ionophores (Nakagawa and others 2000). Treatment of cells with TM resulted in the processing of procaspase-12 (48 kDa) (Fig. 1C). We found that the procaspase-12 level decreased, whereas one of cleaved products increased. We could not detect the prodomain, because caspase-12 antibody used (SIGMA; C7611) here does not recognize the prodomain. Key finding is that the cleavage of procaspase-12 was enhanced in MxA-positive cells upon TM treatment. This result suggests that MxA promotes ER stress-mediated cell death after TM treatment.

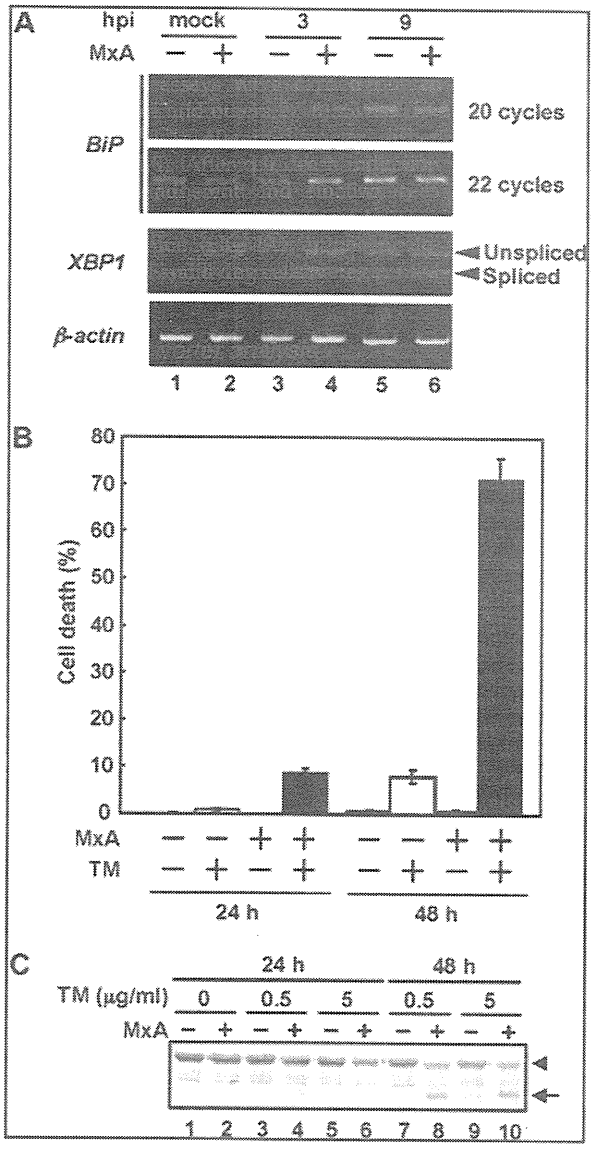

FIG. 1. Cell death is stimulated by TM in cells expressing MxA. **(A)** MxA enhances ER stress caused by influenza virus. Swiss3T3-Neo and Swiss3T3-MxA cells were infected with influenza virus at MOI of 10. After incubation for 3 and 9 h, cells were collected, and the DNA fragment corresponding to *BiP* mRNA was amplified from total RNA by RT-PCR. Resulting products were subjected to 1% agarose gel electrophoresis for *BiP* mRNA (*upper 2 panels*) and *β-actin* mRNA (*lower*) or 8% PAGE for *XBP1* mRNA (*middle*). Unspliced and spliced forms of *XBP1* mRNA were indicated by *arrowheads*. **(B)** Dye exclusion assay. Swiss3T3-Neo (*open columns*) and Swiss3T3-MxA (*filled columns*) cells were treated with TM (0.5 μg/mL). After incubation for 24 and 48 h under cell death induction, cells were collected and subjected to trypan blue dye exclusion assays. **(C)** Cleavage of procaspase-12 upon TM treatment. Swiss3T3-Neo and Swiss3T3-MxA cells were treated with TM (0.5 or 5 μg/mL). After incubation for 24 and 48 h under cell death induction, cells were collected and subjected to western blot analyses with anti-caspase-12 antibody (SIGMA). Procaspase-12 and cleaved forms were indicated by *arrowhead* and *arrow*, respectively. TM, tunicamycin; ER, endoplasmic reticulum; MOI, multiplicity of infection; RT-PCR, reverse transcriptase–polymerase chain reaction.

Promotion of apoptosis mediated by MxA is repressed in the presence of a selective inhibitor of ER stress response

MxA was involved in apoptosis acceleration induced by TM (Fig. 1B, C). However, a rapid accumulation of proteins within ER and collapse of Golgi stacks by treatment of TM or BFA may induce various apoptosis pathways beside ER stress-induced cell death. We examined whether MxA specifically functions in UPR-mediated apoptosis by using a selective inhibitor, Sal. Sal blocks dephosphorylation of eukaryotic translation initiation factor 2 subunit α and protects cells from ER stress-induced apoptosis (Boyce and others 2005).

To determine the effect of Sal on ER stress pathway-specific apoptosis acceleration by MxA, we carried out FACS analyses. As shown in Fig. 2A, we confirmed using the FACS method that cell death is induced by TM treatment and further promoted by MxA. Previously, we showed that cell death is enhanced in MxA-expressing cells when cells were treated with cycloheximide (CHX) or ultraviolet irradiation (Numajiri and others 2006). In this report, we examined the impact of Sal on BFA-induced stress condition (Fig. 2B). Cell death was induced by BFA, and enhanced in cells expressing of MxA. Sal suppressed BFA-induced apoptosis, to some extent, not only in MxA-negative cells, but also in MxA-positive cells. These results suggest that apoptosis acceleration by MxA, at least in part, is caused through ER stress signal pathway.

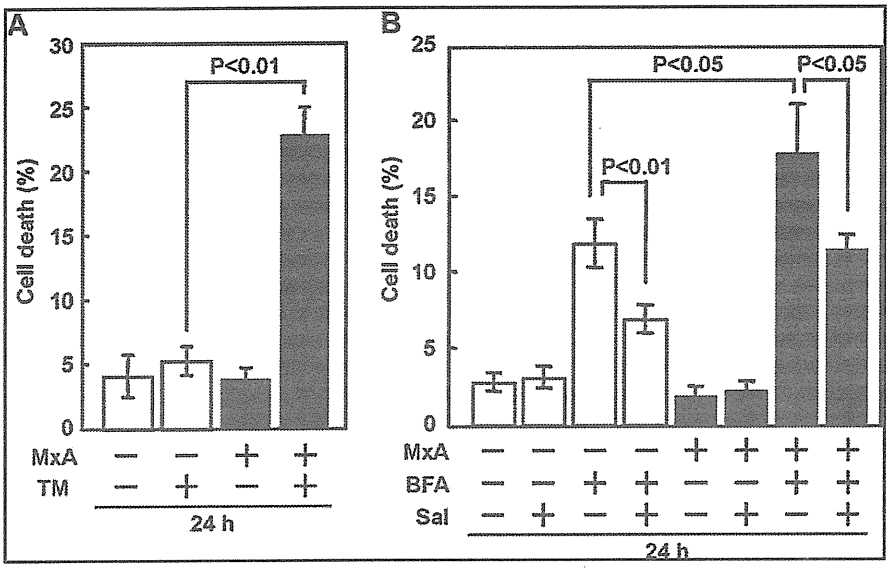

FIG. 2. Sal, a selective ER stress inhibitor suppresses apoptosis accelerated by MxA. (A) Swiss3T3-Neo (*open columns*) and Swiss3T3-MxA (*filled columns*) cells were treated with TM (0.5 μg/mL). After incubation for 24 h, cells were collected and subjected to FACS analysis. (B) Effect of Sal on MxA-induced cell death. Swiss3T3-Neo (*open columns*) and Swiss3T3-MxA (*filled columns*) cells were treated with 50 μM BFA in the presence or absence of 15 μM Sal. After incubation for 24 h, cells were collected and subjected to FACS analysis. Data were presented as means with standard deviation from 3 independent experiments. FACS, fluorescence-activated cell sorting; BFA, Brefeldin A; Sal, Salubrinal.

MxA accelerates UPR after TM treatment

We next examined whether UPR signaling induced by TM is also enhanced in cells expressing MxA. To this end, we examined the mRNA expression level of genes under the control of the UPR signaling. Swiss3T3-MxA and Swiss3T3-Neo cells were treated with TM, and the mRNA level was examined by RT-PCR method. After 6 and 3 h in the presence of 0.5 and 2.5 μg/mL TM, respectively, the *BiP* mRNA level was increased in cells expressing MxA (Fig. 3A, compare lane 5 with lane 6, and lane 7 with lane 8). From 3 h after treatment with 0.5 μg/mL TM, the spliced form of *XBP1* mRNA was detected in cells expressing MxA, whereas this occurred from 12 h after treatment with TM in MxA-negative cells (Fig. 3B). One of the known signals coordinated with ER stress-induced apoptosis is the expression of CHOP (He 2006). As shown in Fig. 3C, after the treatment with 0.5 μg/mL TM, only MxA-positive cells expressed *CHOP* mRNA. Increase of mRNA amount of the gene under the control of the UPR pathway was distinct only in the presence of low concentrations of TM (Fig. 3C, lanes 4 and 6). This MxA-mediated enhancement was not observed when cells were treated with 2.5 μg/mL TM. MxA may not affect ER signaling induced by vast amounts of unfolded proteins. Furthermore, we confirmed that the amount of *CHOP* mRNA is upregulated in cells transiently expressing MxA (Fig. 3D). Collectively, these suggest that MxA reduces the threshold level of ER stress sensing.

We determined whether MxA enhances the transcription promoter activity directed by ERSE or UPRE under the control of UPR. We utilized pGL3-GRP78P(-132)-luc and p5xATF6GL3 plasmids to monitor ERSE- and UPRE-dependent promoter activities, respectively (Zhu and others 1997; Yoshida and others 1998; Wang and others 2000). As shown in Fig. 3E, F, MxA enhanced both ERSE- and UPRE-dependent promoter activities in response to TM treatment. This enhancement by MxA was in a dose-dependent manner and was undetectable when a reporter plasmid pGL3-GRP78Pmut that lacks ERSE was used (data not shown). These results suggest that MxA affects the signaling pathway leading to the transcription activation upon ER stress response or UPR.

MxA interacts with BiP

We showed that MxA enhances both ATF6- and IRE1-dependent activation of ER stress responses. BiP, an ER chaperone, is known to bind to and stabilize these ER stress sensors (He 2006). Therefore, we consider the possibility that MxA interacts with BiP, either directly or indirectly, and depletes this chaperone in the ER stress response. Since majorities of BiP are localized inside of ER, while MxA is in the cytoplasm, we assumed that an additional factor(s) is involved in the BiP and MxA interaction. However, it is reported that some of BiP is also localized in the cytoplasm (Buchkovich and others 2009). In fact, cytoplasmic BiP interacts with caspase-7 and caspase-12 to prevent cell death (Rao and others 2002b).

As shown in Fig. 4A, MxA and BiP were co-localized around ER in cells co-expressing both proteins. Furthermore, the localization pattern of MxA and BiP in uninfected cells was similar to that observed in influenza virus-infected cells (compare with Fig. 4A, B). At 9 hpi, PB1 was present in the nucleus and the cytoplasm (Fig. 4B). In the same cell, MxA and BiP were co-localized in ER and cytoplasm.

To examine whether MxA interacts with BiP *in vivo*, we performed immunoprecipitation assays using lysates prepared from cells transfected with expression plasmids for FLAG-BiP and either HA-MxA wild type (wt) or mutants (Fig. 4C). Western blot analyses revealed that HA-MxAwt was co-immunoprecipitated with FLAG-BiP when anti-FLAG antibody was used (Fig. 4C, lane 10). We used human nucleosome assembly protein-1-L1 (hNAP-1), one of cytoplasmic proteins, as negative control for overexpression condition (Fig. 4C, lanes 1 and 8). In addition, we tried to identify an interaction domain on MxA and binding specificity with BiP. MxAΔC574 lacking zinc finger motif bound to BiP but only weakly, and MxAΔN interacted with BiP a

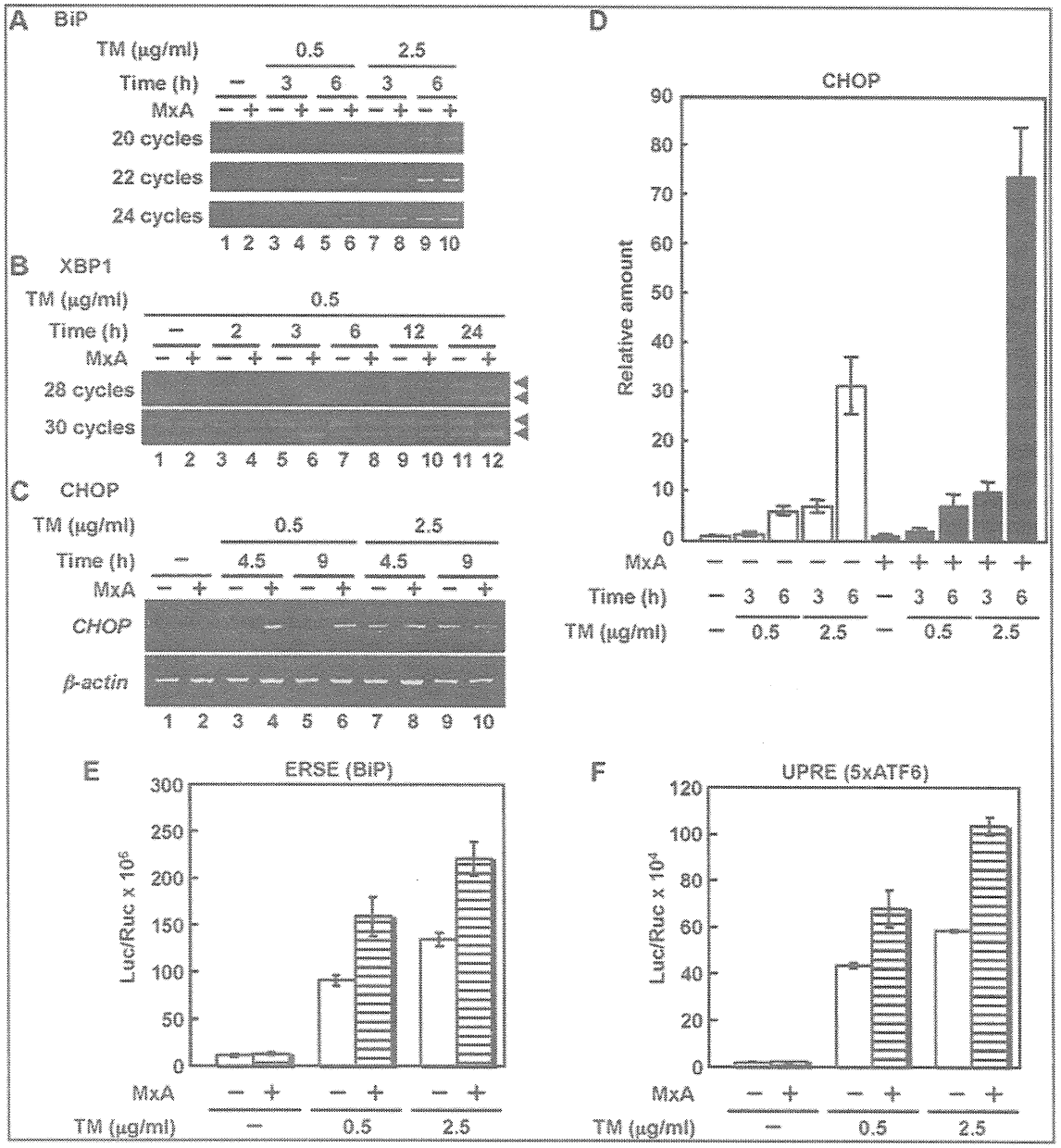

FIG. 3. MxA accelerates UPR after TM treatment. (A–C) Swiss3T3-Neo and Swiss3T3-MxA cells were treated with TM at the indicated concentration. After incubation for indicated time periods, cells were collected, and total RNA were subjected to RT-PCR. Amplified DNA fragments were subjected to separation on 1% agarose gel electrophoresis for *BiP* mRNA (A) and *CHOP* mRNA (C), or 8% PAGE for *XBP1* mRNA (B). Unspliced and spliced forms of *XBP1* mRNA were indicated by *arrowheads*. (D) Quantification of *CHOP* mRNA in MxA-transfected cells using real-time RT-PCR. Swiss3T3 cells were transfected with pCHA or pCHA-MxA plasmid with pBabe-puro. At 24 h post transfection, 2 μg/mL puromycin was added, and cells were grown for further 24 h in growth medium in the presence of 2 μg/mL puromycin. Puromycin-resistant cells were treated with TM at indicated concentrations for 3 and 6 h. (E, F) MxA enhances both ERSE and UPRE. HeLa cells were transfected with pGL3-GRP78P(-132)-luc or p5xATF6GL3 in the presence (*striped columns*) or absence (*open columns*) of an expression plasmid encoding MxA, pCHA-MxA (Mibayashi and others 2002). pRL-SV40 encoding the *Renilla* luciferase was used for internal control. At 24 h after transfection, the cells were treated with or without TM (0.5 or 2.5 μg/mL) for 12 h, and *Firefly* and *Renilla* luciferase activities were measured. The *Firefly* result was normalized by the *Renilla* luciferase activity. UPR, unfolded protein response; ERSE, ER stress response element; UPRE, UPR element.

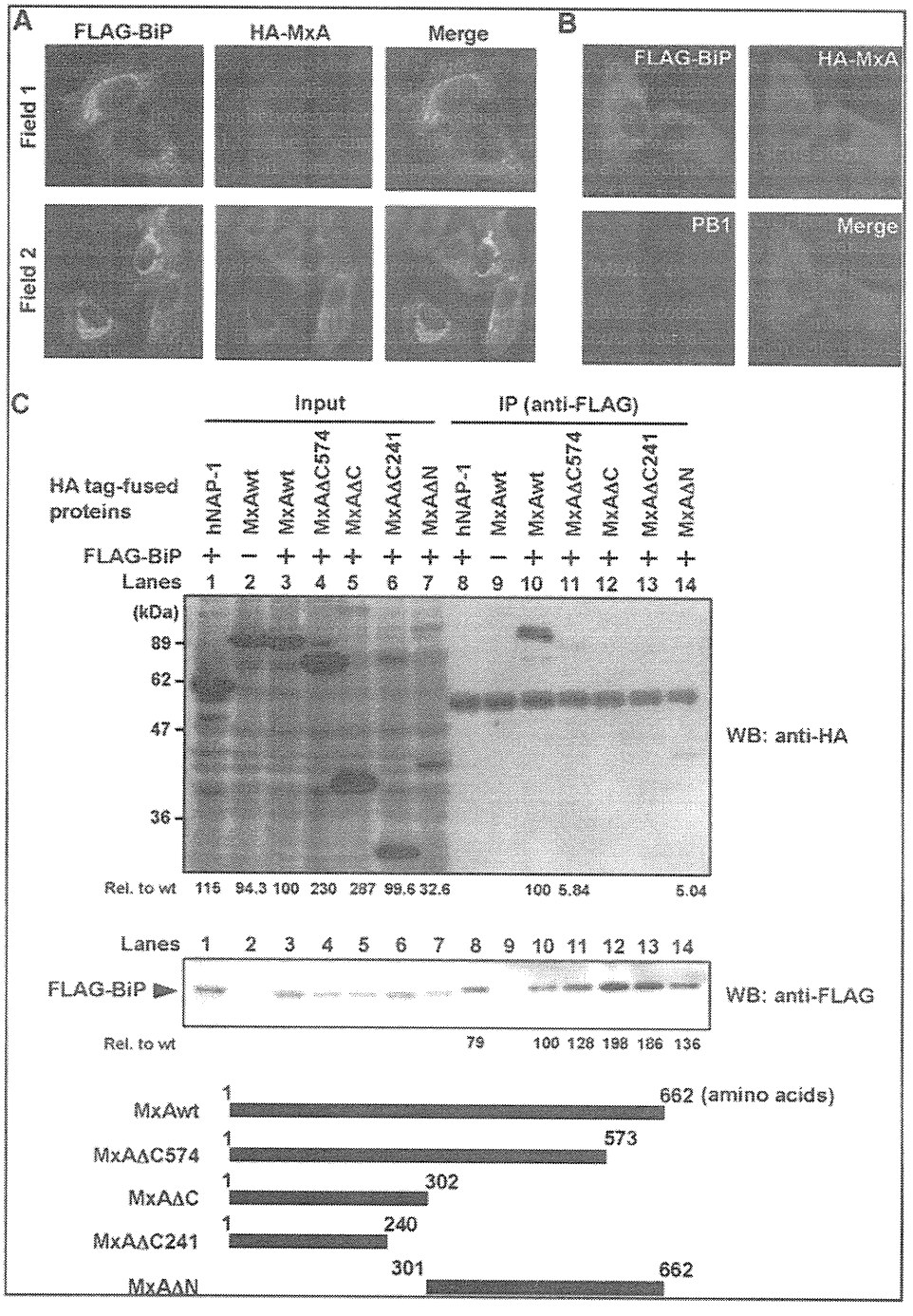

FIG. 4. MxA interacts with BiP. **(A)** Fluorescent immunocytochemical analysis. HeLa cells were transfected with pcDNA-FLAG-BiP and pCHA-MxA, and double-stained with both anti-FLAG and anti-HA antibodies. **(B)** Fluorescent immunocytochemical analysis. HeLa cells were co-transfected with pcDNA3-FLAG-BiP and pCHA-MxA, and at 1 day after transfection, cells were infected with influenza virus at MOI of 10. After incubation for 9 h, cells were collected, and stained with anti-FLAG, anti-HA, and anti-PB1 antibodies. **(C)** Immunoprecipiation assays. HEK293T cells were transfected with pCHA-hNAP-1 (lane 1) or pCHA-MxA mutants (lanes 2–7) in the presence (lanes 1, 3–7) or absence (lane 2) of pcDNA3-FLAG-BiP. Cells were collected at 1 day after transfection, and lysates were subjected to immunoprecipitation assays using anti-FLAG antibody (lanes 8–14). Immunoprecipitated proteins were examined by western blot analyses with anti-HA (*upper panel*) and anti-FLAG antibodies (*lower panel*). Detected protein levels are indicated at the bottom as values relative to those seen in lanes 3 and 10 for the input amount and the immunoprcipitated amount, respectively. MxA mutants used in this assay are schematically illustrated.

little more than MxAΔC574 when compared with the input amounts. However, deletion mutants in the C terminal region, MxAΔC or MxAΔC241 (Fig. 4C, lanes 11 to 14), had virtually no binding capability. Thus, it is quite likely that the region between amino acid positions 301 to 573 of MxA is essential for the binding to BiP. These results indicate that MxA and BiP form a complex around ER. We speculate that this interaction could lead to the activation of ER stress response or the UPR.

BiP suppresses UPR promotion activity of MxA

Finally, we examined whether overexpression of BiP could suppress the ER stress enhancement activity of MxA. We reasoned that either indirect or direct binding of MxA to BiP could be rescued by overexpression of BiP. Reporter gene assays were performed with exogenously overexpressed BiP. Fig. 5A shows that the ER stress response in the absence of TM is not affected by the overexpression of FLAG-BiP. In contrast, in the presence of TM, the activation of ER stress response by MxA was cancelled by overexpressed FLAG-BiP in a dose-dependent manner. Fig. 5B confirmed the expression level of HA-MxA and FLAG-BiP. Thus, it seems likely that ER stress chaperone BiP

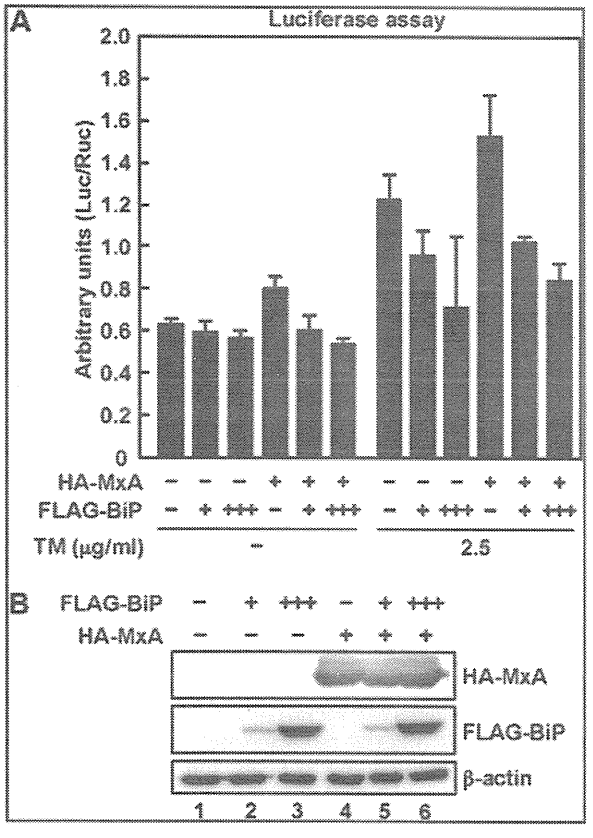

FIG. 5. BiP cancelled UPR promotion activity of MxA. **(A)** Reporter gene assay. HeLa cells were transfected with the reporter plasmid pGL3-GRP78P(-132)-luc with or without pCHA-MxA and pcDNA-FLAG-BiP as described in the figure. At 15 h post transfection, the cells were treated with or without TM (2.5 μg/mL) for 12 h, and the luciferase activity was measured. **(B)** Western blot analyses. Cells treated with TM as shown in **(A)** were subjected to western blot analyses with anti-HA (*upper*), anti-FLAG (*middle*), or anti-β-actin antibodies (*lower*).

cannot be used for its proper role by its depletion through the binding to MxA, either directly or indirectly, on ER membrane. This may reduce the threshold level of ER stress sensing, and thereby promotes the ER stress-induced apoptosis.

Discussion

MxA is an IFN-induced 76 kDa-GTPase that inhibits the multiplication of a variety of RNA viruses, although the exact mechanism of the MxA action is unclear. The antivirus mechanism seems to vary depending on infecting viruses (Schnorr and others 1993; Schneider-Schaulies and others 1994; Landis and others 1998; Gordien and others 2001). When cells expressing MxA are infected with influenza virus, the primary transcription catalyzed by virion-associated viral RNA polymerases occurs at the same level as that in MxA-negative cells (Pavlovic and others 1992). In contrast, viral protein synthesis and genome replication are strongly inhibited (Pavlovic and others 1992). If MxA is forced to be present in the nucleus, nuclear MxA can suppress the influenza virus transcription by interacting with not only the viral polymerase subunit PB2, but also with NP (Turan and others 2004). In addition, we reported that MxA has the cell death promotion activity (Mibayashi and others 2002; Numajiri and others 2006). After influenza virus infection, MxA-positive cells dies faster than MxA-negative cells. We have also shown the caspase-dependent and -independent cell death promotion activity by MxA. It has been reported that the activation of caspase-3 is important during influenza virus proliferation (Queitsch and others 2002). However, the activation level of caspase-3 did not differ between MxA-expressing and MxA-negative cells (Numajiri and others 2006). Therefore, it is possible that MxA could promote cell death without elevation of influenza virus production.

Influenza viruses cause cell death by several mechanisms (Ludwig and others 2006; Sanders and others 2011). Virus infection can induce cell lysis directly, which releases progeny virions and accumulation of a large amount of viral proteins together with potential inflammatory. Promotion of cell death in virus-infected cells may lead to suppression of progeny virion production. The induction of apoptosis might be mediated via intrinsic and/or extrinsic mechanism. It has been shown that viral activation of mitogen-activated protein kinases or their upstream kinases is linked to the onset of apoptosis, and virus infection results in an activation of nuclear factor-κB as an intrinsic pathway. On the other hand, as an extrinsic mechanism of viral apoptosis induction, it has been indicated that the Fas/FasL apoptosis pathway undergoes in a double-stranded RNA activated protein kinase (PKR)-dependent manner in infected cells. The mechanism of viral apoptosis induction might occur via activation of TGF-β, a known apoptosis inducer that is converted from its latent form by NA.

Here, we have addressed the question how MxA promotes cell death after influenza virus infection in light of ER stress signaling. Recent reports suggest that some viruses cause and/or regulate ER stress (Bitko and Barik 2001; Su and others 2002; Tardif and others 2002, 2004; Medigeshi and others 2007). For example, human cytomegalovirus (HCMV) induces splicing of *XBP1* transcript, whereas HCMV suppresses the expression of genes normally regulated by XBP1. It is possible that HCMV utilizes a part of UPR and prevents cell death simultaneously (Isler and others 2005). Dengue

virus envelope protein interacts with BiP and facilitates proper protein folding and protein assembly required for production of progeny virus particles (Limjindaporn and others 2009). In this report, we have shown that MxA enhances ER stress signaling and ER stress-induced cell death upon influenza virus infection. MxA upregulated the transcription level of *BiP* mRNA and the splicing of *XBP1*. MxA also upregulated the transcription level of *CHOP* gene, which is known to be a key mediator for ER stress-induced cell death. Consistent with our findings, CHOP-dependent premature cell death may represent a host defense mechanism to limit viral replication (Medigeshi and others 2007). Previously, we reported that the cell death promotion activity was detected for both MxAwt and MxAΔN, but not for MxΔC in cells treated with CHX as stress inducer. Here, we have shown that the C terminal region on MxA containing oligomelization domain was important in the interaction with BiP. Therefore, similar to the promotion of CHX-induced cell death by MxA, MxA may function as apoptosis accelerator for ER stress-mediated cell death through the same C terminal region.

Previous studies demonstrated that a portion of MxA is localized at membranes belonging to the COP-I-positive subdomain of the smooth ER-Golgi-intermediate compartment (Accola and others 2002; Stertz and others 2006). Furthermore, it has been reported that binding of MxA to viral nucleocapsid protein of La Crosse virus occurs on membranes of the smooth ER-Golgi boundary region and lead to a depletion of the nucleocapsid protein from the viral replication sites (Kochs and others 2002). However, it is presently not clear how MxA interacts with lipid membranes. Anchoring of MxA to distinct membrane compartments may influence the antiviral activity and/or specificity. Recently, Gao and others (2010) reported that the crystal structure of oligomerized stalk region of MxA, which is composed of the middle domain and the GTPase effector domain. The MxA could form a linear oligomers comprised of 13 to 14 dimers. It is not clear how a huge complex of MxA formed through this structure is associated with or incorporated into intracellular membranes. Further studies are needed to clarify details of the connection of MxA-mediated ER stress promotion with antiviral activity.

Acknowledgments

We thank Drs. O. Haller and P. Staeheli (University of Freiburg, Freiburg, Germany), K. Mori (Kyoto University, Kyoto, Japan), and R. Prywes (Columbia University, New York) for their generous gifts of Swiss3T3 and Swiss3T3-MxA cells, and MxA wild-type cDNA, pGL3-GRP78P(-132)-luc, and p5xATF6GL3, respectively. We also thank Dr. Kiong Ho for proofreading the article. This work was supported in part by grants-in-aid from the Ministry of Education, Culture, Sports, Science, and Technology of Japan (T.N. and K.N.).

Author Disclosure Statement

No competing financial interests exist.

References

Accola M, Huang B, Al Masri A, McNiven M. 2002. The antiviral dynamin family member, MxA, tubulates lipids and localizes to the smooth endoplasmic reticulum. J Biol Chem 277:21829–21835.

Bitko V, Barik S. 2001. An endoplasmic reticulum-specific stress-activated caspase (caspase-12) is implicated in the apoptosis of A549 epithelial cells by respiratory syncytial virus. J Cell Biochem 80:441–454.

Boyce M, Bryant KF, Jousse C, Long K, Harding HP, Scheuner D, Kaufman RJ, Ma D, Coen DM, Ron D, Yuan J. 2005. A selective inhibitor of eIF2alpha dephosphorylation protects cells from ER stress. Science 307:935–939.

Buchkovich N, Maguire T, Paton A, Paton J, Alwine J. 2009. The endoplasmic reticulum chaperone BiP/GRP78 is important in the structure and function of the human cytomegalovirus assembly compartment. J Virol 83:11421–11428.

Castelli J, Hassel B, Wood K, Li X, Amemiya K, Dalakas M, Torrence P, Youle R. 1997. A study of the interferon antiviral mechanism: apoptosis activation by the 2-5A system. J Exp Med 186:967–972.

Galluzzi L, Brenner C, Morselli E, Touat Z, Kroemer G. 2008. Viral control of mitochondrial apoptosis. PLoS Pathog 4, e1000018.

Gao S, von der Malsburg A, Paeschke S, Behlke J, Haller O, Kochs G, Daumke O. 2010. Structural basis of oligomerization in the stalk region of dynamin-like MxA. Nature 465:502–506.

García-Sastre A, Biron C. 2006. Type 1 interferons and the virus-host relationship: a lesson in détente. Science 312:879–882.

Gil J, García M, Esteban M. 2002. Caspase 9 activation by the dsRNA-dependent protein kinase, PKR: molecular mechanism and relevance. FEBS Lett 529:249–255.

Gordien E, Rosmorduc O, Peltekian C, Garreau F, Bréchot C, Kremsdorf D. 2001. Inhibition of hepatitis B virus replication by the interferon-inducible MxA protein. J Virol 75:2684–2691.

Haller O, Staeheli P, Kochs G. 2007. Interferon-induced Mx proteins in antiviral host defense. Biochimie 89:812–818.

He B. 2006. Viruses, endoplasmic reticulum stress, and interferon responses. Cell Death Differ 13:393–403.

Hogue BG, Nayak DP. 1992. Synthesis and processing of the influenza virus neuraminidase, a type II transmembrane glycoprotein. Virology 188:510–517.

Hurtley SM, Bole DG, Hoover-Litty H, Helenius A, Copeland CS. 1989. Interactions of misfolded influenza virus hemagglutinin with binding protein (BiP). J Cell Biol 108:2117–2126.

Isler J, Skalet A, Alwine J. 2005. Human cytomegalovirus infection activates and regulates the unfolded protein response. J Virol 79:6890–6899.

Jordan R, Wang L, Graczyk T, Block T, Romano P. 2002. Replication of a cytopathic strain of bovine viral diarrhea virus activates PERK and induces endoplasmic reticulum stress-mediated apoptosis of MDBK cells. J Virol 76:9588–9599.

Kochs G, Janzen C, Hohenberg H, Haller O. 2002. Antivirally active MxA protein sequesters La Crosse virus nucleocapsid protein into perinuclear complexes. Proc Natl Acad Sci U S A 99:3153–3158.

Landis H, Simon-Jödicke A, Klöti A, Di Paolo C, Schnorr J, Schneider-Schaulies S, Hefti H, Pavlovic J. 1998. Human MxA protein confers resistance to Semliki Forest virus and inhibits the amplification of a Semliki Forest virus-based replicon in the absence of viral structural proteins. J Virol 72:1516–1522.

Limjindaporn T, Wongwiwat W, Noisakran S, Srisawat C, Netsawang J, Puttikhunt C, Kasinrerk W, Avirutnan P, Thiemmeca S, Sriburi R, Sittisombut N, Malasit P, Yenchitsomanus P. 2009. Interaction of dengue virus envelope protein with endoplasmic reticulum-resident chaperones facilitates dengue virus production. Biochem Biophys Res Commun 379:196–200.

Ludwig S, Pleschka S, Planz O, Wolff T. 2006. Ringing the alarm bells: signalling and apoptosis in influenza virus infected cells. Cell Microbiol 8:375–386.

Maruoka S, Hashimoto S, Gon Y, Nishitoh H, Takeshita I, Asai Y, Mizumura K, Shimizu K, Ichijo H, Horie T. 2003. ASK1 regulates influenza virus infection-induced apoptotic cell death. Biochem Biophys Res Commun 307:870–876.

Medigeshi G, Lancaster A, Hirsch A, Briese T, Lipkin W, Defilippis V, Früh K, Mason P, Nikolich-Zugich J, Nelson J. 2007. West Nile virus infection activates the unfolded protein response, leading to CHOP induction and apoptosis. J Virol 81:10849–10860.

Mibayashi M, Nakad K, Nagata K. 2002. Promoted cell death of cells expressing human MxA by influenza virus infection. Microbiol Immunol 46:29–36.

Morishima N, Nakanishi K, Takenouchi H, Shibata T, Yasuhiko Y. 2002. An endoplasmic reticulum stress-specific caspase cascade in apoptosis. Cytochrome c-independent activation of caspase-9 by caspase-12. J Biol Chem 277:34287–34294.

Morris SJ, Price GE, Barnett JM, Hiscox SA, Smith H, Sweet C. 1999. Role of neuraminidase in influenza virus-induced apoptosis. J Gen Virol 80 (Pt 1):137–146.

Morris SJ, Smith H, Sweet C. 2002. Exploitation of the Herpes simplex virus translocating protein VP22 to carry influenza virus proteins into cells for studies of apoptosis: direct confirmation that neuraminidase induces apoptosis and indications that other proteins may have a role. Arch Virol 147:961–979.

Naito T, Momose F, Kawaguchi A, Nagata K. 2007. Involvement of Hsp90 in assembly and nuclear import of influenza virus RNA polymerase subunits. J Virol 81:1339–1349.

Nakagawa T, Zhu H, Morishima N, Li E, Xu J, Yankner B, Yuan J. 2000. Caspase-12 mediates endoplasmic-reticulum-specific apoptosis and cytotoxicity by amyloid-beta. Nature 403:98–103.

Numajiri A, Mibayashi M, Nagata K. 2006. Stimulus-dependent and domain-dependent cell death acceleration by an IFN-inducible protein, human MxA. J Interferon Cytokine Res 26: 214–219.

Okuwaki M, Kato K, Nagata K. 2010. Functional characterization of human nucleosome assembly protein 1-like proteins as histone chaperones. Genes Cells 15:13–27.

Pavlovic J, Haller O, Staeheli P. 1992. Human and mouse Mx proteins inhibit different steps of the influenza virus multiplication cycle. J Virol 66:2564–2569.

Postigo A, Ferrer P. 2009. Viral inhibitors reveal overlapping themes in regulation of cell death and innate immunity. Microbes Infect 11:1071–1078.

Queitsch C, Sangster TA, Lindquist S. 2002. Hsp90 as a capacitor of phenotypic variation. Nature 417:618–624.

Rao R, Castro-Obregon S, Frankowski H, Schuler M, Stoka V, del Rio G, Bredesen D, Ellerby H. 2002a. Coupling endoplasmic reticulum stress to the cell death program. An Apaf-1-independent intrinsic pathway. J Biol Chem 277:21836–21842.

Rao R, Peel A, Logvinova A, del Rio G, Hermel E, Yokota T, Goldsmith P, Ellerby L, Ellerby H, Bredesen D. 2002b. Coupling endoplasmic reticulum stress to the cell death program: role of the ER chaperone GRP78. FEBS Lett 514:122–128.

Sadler A, Williams B. 2008. Interferon-inducible antiviral effectors. Nat Rev Immunol 8:559–568.

Sanders CJ, Doherty PC, Thomas PG. 2011. Respiratory epithelial cells in innate immunity to influenza virus infection. Cell Tissue Res 343:13–21.

Schneider-Schaulies S, Schneider-Schaulies J, Schuster A, Bayer M, Pavlovic J, ter Meulen V. 1994. Cell type-specific MxA-mediated inhibition of measles virus transcription in human brain cells. J Virol 68:6910–6917.

Schnorr J, Schneider-Schaulies S, Simon-Jödicke A, Pavlovic J, Horisberger M, ter Meulen V. 1993. MxA-dependent inhibition of measles virus glycoprotein synthesis in a stably transfected human monocytic cell line. J Virol 67:4760–4768.

Schultz-Cherry S, Hinshaw VS. 1996. Influenza virus neuraminidase activates latent transforming growth factor beta. J Virol 70:8624–8629.

Staeheli P, Haller O, Boll W, Lindenmann J, Weissmann C. 1986. Mx protein: constitutive expression in 3T3 cells transformed with cloned Mx cDNA confers selective resistance to influenza virus. Cell 44:147–158.

Stertz S, Reichelt M, Krijnse-Locker J, Mackenzie J, Simpson J, Haller O, Kochs G. 2006. Interferon-induced, antiviral human MxA protein localizes to a distinct subcompartment of the smooth endoplasmic reticulum. J Interferon Cytokine Res 26:650–660.

Stray SJ, Air GM. 2001. Apoptosis by influenza viruses correlates with efficiency of viral mRNA synthesis. Virus Res 77:3–17.

Su H, Liao C, Lin Y. 2002. Japanese encephalitis virus infection initiates endoplasmic reticulum stress and an unfolded protein response. J Virol 76:4162–4171.

Tardif K, Mori K, Kaufman R, Siddiqui A. 2004. Hepatitis C virus suppresses the IRE1-XBP1 pathway of the unfolded protein response. J Biol Chem 279:17158–17164.

Tardif K, Mori K, Siddiqui A. 2002. Hepatitis C virus subgenomic replicons induce endoplasmic reticulum stress activating an intracellular signaling pathway. J Virol 76:7453–7459.

Timofeeva TA, Klenk ND, Zhirnov OP. 2001. [Identification of the protease-binding domain in the N-terminal region of the influenza A virus matrix protein M1]. Mol Biol (Mosk) 35:484–491.

Turan K, Mibayashi M, Sugiyama K, Saito S, Numajiri A, Nagata K. 2004. Nuclear MxA proteins form a complex with influenza virus NP and inhibit the transcription of the engineered influenza virus genome. Nucleic Acids Res 32:643–652.

Urano F, Wang X, Bertolotti A, Zhang Y, Chung P, Harding H, Ron D. 2000. Coupling of stress in the ER to activation of JNK protein kinases by transmembrane protein kinase IRE1. Science 287:664–666.

Wang Y, Shen J, Arenzana N, Tirasophon W, Kaufman R, Prywes R. 2000. Activation of ATF6 and an ATF6 DNA binding site by the endoplasmic reticulum stress response. J Biol Chem 275:27013–27020.

Yoshida H, Haze K, Yanagi H, Yura T, Mori K. 1998. Identification of the cis-acting endoplasmic reticulum stress response element responsible for transcriptional induction of mammalian glucose-regulated proteins. Involvement of basic leucine zipper transcription factors. J Biol Chem 273:33741–33749.

Zamarin D, García-Sastre A, Xiao X, Wang R, Palese P. 2005. Influenza virus PB1-F2 protein induces cell death through mitochondrial ANT3 and VDAC1. PLoS Pathog 1:e4.

Zhirnov OP, Konakova TE, Garten W, Klenk H. 1999. Caspase-dependent N-terminal cleavage of influenza virus nucleocapsid protein in infected cells. J Virol 73:10158–10163.

Zhu C, Johansen F, Prywes R. 1997. Interaction of ATF6 and serum response factor. Mol Cell Biol 17:4957–4966.

Address correspondence to:
Prof. Kyosuke Nagata
Department of Infection Biology
Graduate School of Comprehensive Human Sciences
University of Tsukuba
1-1-1 Tennodai
Tsukuba 305-8575
Japan

E-mail: knagata@md.tsukuba.ac.jp

Received 28 September 2010/Accepted 5 July 2011

JOURNAL OF VIROLOGY, Aug. 2011, p. 7504–7512
0022-538X/11/$12.00 doi:10.1128/JVI.02375-10

Vol. 85, No. 15

Recognition of Cap Structure by Influenza B Virus RNA Polymerase Is Less Dependent on the Methyl Residue than Recognition by Influenza A Virus Polymerase▽†

Chitose Wakai,[1,2] Minako Iwama,[2] Kiyohisa Mizumoto,[2,3] and Kyosuke Nagata[1]*

Department of Infection Biology, Graduate School of Comprehensive Human Sciences, University of Tsukuba, 1-1-1 Tennodai, Tsukuba 305-8575, Japan[1]; Department of Biochemistry, School of Pharmaceutical Sciences, Kitasato University, 5-9-1 Shirokane, Minato-ku, Tokyo 108-8641, Japan[2]; and Microbial Chemistry Research Center, 3-14-23 Kamiosaki, Shinagawa-ku, Tokyo 141-0021, Japan[3]

Received 12 November 2010/Accepted 10 May 2011

The cap-dependent endonuclease activity of the influenza virus RNA-dependent RNA polymerase cleaves host mRNAs to produce capped RNA fragments for primers to initiate viral mRNA synthesis. The influenza A virus (FluA) cap-dependent endonuclease preferentially recognizes the cap1 structure (m^7GpppNm). However, little is known about the substrate specificity of the influenza B virus (FluB) endonuclease. Here, we determined the substrate specificity of the FluB polymerase using purified viral RNPs and ^{32}P-labeled polyribonucleotides containing a variety of cap structures (m^7GpppGm, m^7GpppG, and GpppG). We found that the FluA polymerase cleaves m^7G-capped RNAs preferentially. In contrast, the FluB polymerase could efficiently cleave not only m^7G-capped RNAs but also unmethylated GpppG-RNAs. To identify a key amino acid(s) related to the cap recognition specificity of the PB2 subunit, the transcription activity of FluB polymerases containing mutated cap-binding domains was examined by use of a minireplicon assay system. In the case of FluA PB2, Phe323, His357, and Phe404, which stack the m^7GTP, and Glu361 and Lys376, which make hydrogen bonds with a guanine base, were essential for the transcription activity. In contrast, in the case of FluB PB2, the stacking interaction of Trp359 with a guanine base and putative hydrogen bonds using Gln325 and Glu363 were enough for the transcription activity. Taking these results together with the result for the cap-binding activity, we propose that the cap recognition pocket of FluB PB2 does not have the specificity for m^7G-cap structures and thus is more flexible to accept various cap structures than FluA PB2.

Influenza A virus (FluA) and influenza B virus (FluB) belong to the family of *Orthomyxoviridae*. The genomes of FluA and FluB are composed of a set of eight segments of RNA (vRNA) of negative polarity. vRNA is complexed with nucleoprotein (NP) and associated with the RNA polymerase to form viral ribonucleoprotein (vRNP) complexes. vRNP is an essential unit for both transcription and replication (9). In transcription, the RNA polymerase catalyzes not only RNA polymerization and polyadenylation of mRNA but also cleavage of host mRNAs to generate capped RNA fragments. The RNA polymerase is composed of one molecule each of three viral proteins, PB1, PB2, and PA. PB1 plays central roles in both RNA polymerase assembly (27, 31) and RNA polymerization (6). It contains the conserved motifs characteristic of RNA-dependent RNA polymerases and is directly involved in RNA chain elongation (1, 2). It binds to 5′- and 3′-terminal sequences of vRNA and cRNA (cRNA to vRNA), which are conserved in all segments and act as *cis*-acting elements for the viral RNA synthesis. PB2 is required for transcription and binds to the cap structures of host mRNAs. Recently, the structural features of the cap-binding site in FluA PB2 and the FluA PB1-PB2 contact site have been determined by functional studies and crystallography (12, 31). PA is involved in not only virus genome replication but also transcription as an endonuclease for generation of primers for RNA synthesis (8, 10, 13, 19, 36). It is also reported that PA is important for the polymerase assembly (19). The structure of the PB1-PA contact site has also been determined crystallographically (14, 27).

The FluA polymerase exhibits a cap-dependent endonuclease activity, which cleaves host mRNAs to produce capped RNA fragments with lengths of 11 to 13 nucleotides (nt). The resulting capped RNA fragment serves as a primer to initiate viral mRNA synthesis. It is well known that in the case of the FluA polymerase, eukaryotic mRNAs containing m^7G(5′)ppp(5′)Nm (cap1) and m^7G(5′)ppp(5′)NmN′m (cap2) structures stimulate *in vitro* viral RNA transcription strongly (4, 5, 29). Removal of m^7G of the cap from mRNA eliminates the priming activity, and naturally occurring uncapped mRNAs do not prime transcription (5, 29). In addition, the presence of methyl groups in the cap is required for the priming activity; reovirus mRNAs with 5′-terminal GpppG are inactive as primers (3). It has also been demonstrated that each of the two methyl groups in the cap1 structure, the 7-methyl residue of guanine and the 2′-*O*-methyl on the ribose of guanosine, strongly influences the capped RNA-primed transcription activity (4).

Biochemical and structural studies revealed the functional structures of the cap-binding proteins, including FluA PB2 (12), human translation initiation factor 4E (eIF4E) (33, 34),

* Corresponding author. Mailing address: Department of Infection Biology, Graduate School of Comprehensive Human Sciences, University of Tsukuba, 1-1-1 Tennodai, Tsukuba 305-8575, Japan. Phone and fax: 81-29-853-3233. E-mail: knagata@md.tsukuba.ac.jp.

† Supplemental material for this article may be found at http://jvi.asm.org/.

▽ Published ahead of print on 18 May 2011.

human nuclear cap-binding protein 20 (CBP20) (23), and vaccinia virus (nucleoside-2′-*O*-)-methyltransferase (VP39) (16). The overall structures of these four cap-binding proteins differ widely due to their evolutionarily unrelated origins, but the cap-binding pockets form a common structure and preferentially bind to the 7-methylated cap structure. These cap-binding proteins hardly bind to the unmethylated cap structure.

Most of our knowledge on the transcription mechanism of the influenza virus genome has been derived from studies on the FluA polymerase, whereas little is known about the FluB polymerase. It is reported that α-amanitin, a potent inhibitor for the host cell RNA polymerase II, inhibits influenza virus transcription, suggesting that eukaryotic mRNAs containing the cap structure are essential for influenza virus transcription (21). Using α-amanitin, we found that the growth of FluB is more sensitive to the amount of cellular mRNA than that of FluA (data not shown). To elucidate the transcription initiation mechanism of the FluB polymerase, we tried to determine the specificity of cap recognition by the FluB polymerase. First, we compared the substrate specificities of FluA and FluB polymerases using purified vRNPs and various capped RNA substrates (m^7GpppGm-, m^7GpppG-, and GpppG-RNA) and found that the FluB polymerase efficiently cleaves not only m^7G-capped RNAs but also unmethylated GpppG-RNA, whereas the FluA polymerase cleaves m^7G-capped RNAs specifically. We then tried to identify key amino acids related to the cap recognition of FluB PB2. In order to examine the transcription activity using mutated PB2 proteins, we utilized FluA and FluB minireplicon assay systems using a virus polymerase-dependent reporter gene (17, 35). The minireplicon system has been utilized for a number of functional analyses of *cis*-acting elements with the viral genome and *trans*-acting viral factors (10, 35). The reporter gene contains a coding region flanked by each viral 5′ and 3′ untranslated region (UTR), which function as promoters, and therefore mimics an influenza virus genomic segment. Using this assay system, we identified the important amino acids required for the cap recognition by the FluB polymerase by referencing functionally important amino acids in the FluA polymerase (12).

Based on the findings using the assay systems, we propose that the FluB polymerase possesses a novel cap recognition mechanism, which is different not only from the FluA polymerase but also from well-known cap-binding proteins. These findings could be important to develop novel anti-influenza virus drugs targeting the cap recognition and cleavage reaction.

MATERIALS AND METHODS

Biological materials. Monolayer cultures of 293T and MDCK cells were maintained at 37°C in Dulbecco's modified Eagle medium (DMEM) and minimal essential medium (MEM) (Nissui), respectively, supplemented with 10% fetal calf serum (Cell Culture Technologies). Influenza virus A/Panama/2007/99 (A/PA/99) and B/Shanghai/361/2002 (B/SH/02) were kindly supplied by Y. Suzuki and T. Gotanda (Kitasato Institute, Research Center for Biologicals, Saitama, Japan). Vaccinia virus capping enzyme and recombinant human mRNA (guanine-7-)methyltransferase (rhMTase) were prepared according to a previously described procedure (28).

Cloning of cDNAs for viral RNA polymerase subunits and nucleoprotein cDNA. For construction of mammalian expression vectors for influenza virus polymerase subunits (PB1, PB2, and PA) and nucleoprotein (NP), cDNAs corresponding to the full-length PB1, PB2 with a FLAG tag at its C terminus (PB2cFLAG), PA, and NP were amplified by reverse transcription-PCR (RT-PCR) from vRNAs of influenza virus A/PA/99 and B/SH/02 as templates using the following sets of phosphorylated primers (see Table S1 in the supplemental material): A-PB1-FOR and A-PB1-REV for FluA-PB1, A-PB2-FOR and A-PB2-cFLAG-REV for FluA-PB2cFLAG, A-PA-FOR and A-PA-REV for FluA-PA, A-NP-FOR and A-NP-REV for FluA-NP, B-PB1-FOR and B-PB1-REV for FluB-PB1, B-PB2-FOR and B-PB2-cFLAG-REV for FluB-PB2cFLAG, B-PA-FOR and B-PA-REV for FluB-PA, and B-NP-FOR and B-NP-REV for FluB-NP. The PCR products were then cloned into the EcoRV site of pCAGGS-P7 (7), resulting in construction of pCAGGS-Panama-PB1, pCAGGS-Panama-PB2-cFLAG, pCAGGS-Panama-PA, pCAGGS-Panama-NP, pCAGGS-Shanghai-PB1, pCAGGS-Shanghai-PB2-cFLAG, pCAGGS-Shanghai-PA, and pCAGGS-Shanghai-NP. cDNAs for PB2 mutants were prepared by site-directed mutagenesis using the primer sets for FluA-PB2-cFLAG and FluB-PB2-cFLAG and mutant primer sets (see Table S2 in the supplemental material). The PB2 mutant genes have been fully sequenced by standard methods (35).

Preparation of influenza virus vRNP. To prepare vRNP, we first treated purified influenza virus virions at 30°C for 60 min with a disruption buffer consisting of 50 mM Tris-HCl (pH 8.0), 100 mM KCl, 5 mM $MgCl_2$, 1 mM dithiothreitol (DTT), 5% glycerol, 2% Triton X-100, and 2% lysolecithin according to a method described previously (32). The sample was then directly subjected to centrifugation on a 30 to 60% (wt/vol) linear gradient of glycerol on a 70% (wt/vol) glycerol cushion in 50 mM Tris-HCl (pH 8.0) and 150 mM NaCl in a Beckman MLS-50 rotor with adapters at 163,000 × g_{AV} for 3 h at 4°C. Fractionation was carried out from the top of the gradient. Fractions containing vRNP were pooled and then used for *in vitro* endonuclease and elongation assays.

Preparation of various RNA substrates. Triphosphate-ended RNA with the 33-nucleotide sequence 5′-GAAAAAAAAAAAAAAAAAAAAAAAAAAAAAAAA UAAA-3′, designated pppG-RNA, was synthesized by using T7 RNA polymerase (Amersham Biosciences) and a synthetic DNA template. The protocol was previously described (30). Briefly, to prepare the template for the T7 RNA polymerase, the oligonucleotide T7P (5′-TAATACGACTCACTATA-3′), corresponding to the T7 promoter (−17 to −1), was annealed to the template oligonucleotide T7-polyA-R1 (5′-TTTATTTTTTTTTTTTTTTTTTTTTTTTTTT TTCTATAGTGAGTCGTATTA-3′, where the underlined sequence is complementary to the T7 promoter [−17 to −1]). After the transcription reaction, the transcription mixture was treated with DNase I (Roche Applied Science). RNA was then extracted with phenol-chloroform, ethanol precipitated, and used as a capping substrate. To synthesize m^7G[^{32}P]pppGm-RNA and G[^{32}P]pppG-RNA, 50 pmol of pppG-RNA was incubated at 37°C for 2 h in the presence of 8 μM [α-^{32}P]GTP (800 cpm/fmol) and an appropriate amount of purified vaccinia virus capping enzyme, which has guanylyltransferase, guanine-7-methyltransferase, and ribose-2′-*O*-methyl-transferase activities, in a reaction mixture (50 μl) containing 50 mM Tris-HCl (pH 7.9), 2 mM $MgCl_2$, 40 mM NaCl, and 20 mM DTT in the presence or absence of 150 μM *S*-adenosyl-L-methionine (AdoMet). After the reaction, capped RNA was extracted with phenol-chloroform, ethanol precipitated, and dissolved in H_2O. To synthesize m^7G[^{32}P]pppG-RNA, 0.4 pmol of G[^{32}P]pppG-RNA was incubated at 30°C for 20 min with 15 ng/μl of rhMTase in a reaction mixture (20 μl) containing 25 mM Tris-HCl (pH 7.9), 0.5 mM DTT, 0.1 mg/ml bovine serum albumin (BSA), and 50 μM AdoMet. The RNA was extracted with phenol-chloroform, ethanol precipitated, and dissolved in H_2O. To confirm the cap structure on the synthesized RNA, the cap structure of the synthesized ^{32}P-capped RNA was liberated by digestion with nuclease P_1 (Wako) (28). The reaction product was analyzed by thin-layer chromatography (TLC) on a polyethyleneimine (PEI)-cellulose plate (PEI-CEL UV_{254}; Macherey-Nagel) with 0.65 M LiCl and visualized by autoradiography.

***In vitro* capped RNA cleavage and RNA elongation reactions.** The determination of Flu cap-dependent endonuclease activity and the subsequent RNA elongation reaction were carried out in a reaction mixture (25 μl) containing 50 mM Tris-HCl (pH 7.9), 0.1 mM ammonium acetate, 5 mM $MgCl_2$, 2.5 mM DTT, 0.1% Nonidet P-40, 8 U of RNasin, 3 to 5 fmol of each ^{32}P-capped RNA (800 cpm/fmol), and an appropriate amount of purified vRNPs without or with ATP, UTP, GTP, or CTP. The reaction mixture was incubated at 30°C for 2 h, and then RNA products were extracted with phenol-chloroform and ethanol precipitated. The RNA products denatured with formamide were electrophoresed in a 20% acrylamide gel containing 8 M urea. After electrophoresis, the gel was dried, and RNAs were visualized by autoradiography. The amount of synthesized RNA was measured with a liquid scintillation counter (LS6000IC; Beckman). The endonuclease activity was represented as a ratio of the amount of cleaved RNAs to that of total capped RNAs, and the RNA elongation efficiency was represented as a ratio of the amount of transcripts to that of total capped RNAs.

Cap-binding assay. UV cross-linking was carried out to measure the cap-binding activity of viral RNA polymerases. A reaction mixture (12 μl) containing

50 mM Tris-HCl (pH 7.9), 0.1 mM ammonium acetate, 5 mM $MgCl_2$, 2.5 mM DTT, 250 fmol of uncapped RNA substrate, 50 fmol of each ^{32}P-capped RNA (~800 cpm/fmol), and an appropriate amount of purified vRNPs was incubated for 30 min on ice and then irradiated on ice for 10 min with 254-nm UV light (FUNA-UV-Linker FS-1500 [Funakoshi, Japan]) with 0.2 mg/ml of heparin. The ^{32}P-labeled products were digested with nuclease P_1, analyzed by 6% SDS-PAGE, and detected by autoradiography.

Minireplicon assay. Two plasmid vectors carrying a reporter gene (an artificial influenza virus genome containing the firefly luciferase gene of negative polarity, which is synthesized in cells by the human DNA-dependent RNA polymerase I [Pol I]), were constructed as described previously (35). A fragment containing the luciferase gene sandwiched by 5′- and 3′-terminal sequences of FluA/PA/99 and FluB/SH/02 segment 8 was amplified by PCR with specific primers 5′-GTAGTAGAAACAAGGGTGTTTTTTACTCGAGATCTTACAATTTGGACTTTCCGCCCTT-3′ and 5′-GATCCGTCTCCGGGAGCAAAAGCAGGGTGACAAAGACATAATGCATATGGAAGACGCCAAAAACATAAAGAAAGG-3′ for FluA/PA/99 and 5′-TATTCGTCTCAGGGAGCAGAAGCAGAGGATTTGTTTAGTCACTGGCAAACGGAAAAAAATGGAAGACGCCAAAAACATAAAG-3′ and 5′-ATATCGTCTCGTATTAGTAGTAACAAGAGGATTTTTATTTTAAATTTACAATTTGGACTTTCCGCC-3′ for FluB/SH/02, using pGV-B (the promoterless luciferase reporter vector; Toyo Inc.) as a template. The amplified PCR products were digested with BsmBI and cloned into pHH21 containing the promoter region of the human rRNA gene (24, 25), which had been digested with BsmBI. The constructed plasmids were designated pHH-A-vNS-Luc and pHH-B-vNS-Luc, in which the luciferase gene in reverse orientation sandwiched with 23- and 26-nucleotide 5′- and 3′-terminal sequences of the FluA/PA/99 segment 8 or 30 and 44-nucleotide 5′- and 3′-terminal sequences of the FluB/SH/02 segment 8, respectively, is placed under the control of the human Pol I promoter. 293T cells were transfected with plasmids for the expression of the FluA minireplicon (pCAGGS-Panama-PB1, pCAGGS-Panama-PB2-cFLAG, pCAGGS-Panama-PA, pCAGGS-Panama-NP, and pHH-A-vNS-Luc) or FluB minireplicon (pCAGGS-Shanghai-PB1, pCAGGS-Shanghai-PB2-cFLAG, pCAGGS-Shanghai-PA, pCAGGS-Shanghai-NP, and pHH-B-vNS-Luc). A plasmid for the expression of *Renilla* luciferase driven by the simian virus 40 (SV40) promoter was used as an internal control for the dual-luciferase assay. As a negative control, 293T cells were transfected with the same plasmids, except for the omission of the PB2 expression plasmid. After transfection, the cells were incubated at 37°C for 24 h, and then the luciferase activity was determined using commercially available reagents (Promega) according to the manufacturer's protocol. The relative luminescence intensity was measured with a luminometer for 20 s. To measure the levels of accumulation of viral mRNA, cRNA, and vRNA, quantitative RT-PCR was performed. Total RNA was extracted from transfected cells and then reverse transcribed with either (i) oligo$(dT)_{20}$ for synthesizing cDNA from viral mRNA, (ii) 5′-ATATCGTCTCGTATTAGTAGTAACAAGAGCATT-3′, which is complementary to the 3′ portion of cRNA of the reporter gene, for synthesizing cDNA from cRNA, or (iii) 5′-TCCATCACGGTTTTGGAATGTTTACTACAC-3′, which is complementary to vRNA, for synthesizing cDNA from vRNA of the reporter gene. These single-stranded cDNAs were subjected to real-time quantitative PCR analyses (Thermal Cycler Dice real-time system TP800; TaKaRa) with SYBR Premix Ex *Taq* (TaKaRa) and two specific primers, 5′-TCCATCACGGTTTTGGAATGTTTACTACAC-3′, corresponding to the firefly luciferase mRNA between nucleotide sequence positions 728 and 757, and 5′-GTGCGCCCCCAGAAGCAATTTC-3′, which is complementary to the firefly luciferase mRNA between nucleotide sequence positions 931 and 952. *Renilla* luciferase mRNA was also amplified with two specific primers, 5′-GCAGCATATCTTGAACCATTC-3′, corresponding to the *Renilla* luciferase mRNA between nucleotide sequence positions 598 and 618, and 5′-CATCACTTGCACGTAGATAAG-3′, which is complementary to the *Renilla* luciferase mRNA between nucleotide sequence positions 725 and 745. The relative amounts of mRNA, cRNA, and vRNA were calculated by using the second-derivative maximum method and normalized to the amount of *Renilla* luciferase mRNA. The ratio of the amounts of mRNA and cRNA relative to vRNA is shown.

Detection of capped RNA coprecipitated with the viral RNA polymerase. 293T cells were transfected with plasmids for the expression of the FluB viral proteins, PB1, FLAG-tagged PB2 (wild-type or mutated PB2), and PA. At 24 h posttransfection, cells were resuspended in a lysis buffer (20 mM Tris-HCl [pH 7.9], 100 mM NaCl, 30 mM KCl, and 0.1% Nonidet P-40). The RNA polymerase complex composed of PB1, FLAG-tagged PB2, and PA was purified by incubation with anti-FLAG M2 agarose (Sigma) at 4°C for 3 h and eluted with an elution buffer (50 mM Tris-HCl [pH 7.9], 100 mM ammonium acetate, 5 mM $MgCl_2$, and 10% [vol/vol] glycerol) containing 0.1 mg/ml FLAG peptide (Sigma). RNAs which interact with the viral RNA polymerase was extracted from recombinant RNA polymerase complexes (100 ng of PB1 equivalents) with phenol-chloroform and ethanol precipitated with 20 μg of carrier tRNA. After treatment with calf intestinal alkaline phosphatase (CIAP), which removes free phosphate groups, periodate oxidation under mild conditions followed by β-elimination with aniline was carried out to remove 5′-terminal m^7G from capped RNA, generating RNA with 5′-triphosphate, which is the substrate for vaccinia virus capping enzyme, as described previously (4, 11). The RNA was then recapped using vaccinia virus capping enzyme with [α-^{32}P]GTP as described in the previous section. To measure the amount of ^{32}P-labeled capped RNA, the RNA was digested with tobacco acid pyrophosphatase (TAP) (Sigma) at 37°C for 1 h in a buffer containing 50 mM sodium acetate (pH 5.5), 5 mM EDTA, and 10 mM 2-mercaptoethanol. The reaction product was analyzed by thin-layer chromatography on a PEI-cellulose plate as described above, and the amount of [^{32}P]m^7Gp was measured with a liquid scintillation counter.

RESULTS

***In vitro* capped RNA cleavage reaction and subsequent RNA elongation reaction.** The FluA polymerase requires the cap1 structure ($m^7GpppNm$) stringently for transcription (4). In contrast, little is known about the requirement for the cap structure of the FluB polymerase. Thus, we first examined the efficiency of the capped RNA cleavage reaction and subsequent RNA elongation reaction by FluA and FluB polymerases using cap1-RNA ($m^7GpppGm$-RNA). The cap1-RNA labeled with ^{32}P in the cap structure was incubated with purified vRNP (see Fig. S1A in the supplemental material) in the absence or presence of nucleoside triphosphates (NTPs) (Fig. 1A). RNA products were analyzed by 15% PAGE containing 8 M urea. FluA and FluB polymerases cleaved the cap1-RNA and produced 11- to 13-nucleotide and 11- to 12-nucleotide RNAs, respectively, in the absence of NTPs (Fig. 1A, lanes 2 to 7), indicating that the endonuclease activity of FluB is different from that of FluA in the distance of cleavage site from the cap structure. This cleavage pattern was observed commonly among FluA strains and among FluB strains (see Fig. S1B, lanes 2 to 6, in the supplemental material). The cleaved RNA products were elongated in the presence of NTPs in a dose-dependent manner (Fig. 1A, lanes 8 to 13), but the elongation efficiency of the FluB polymerase was lower than that of the FluA polymerase. We also confirmed that these elongated products contain full-length transcripts from 8 segments and are partially polyadenylated (see Fig. S2 in the supplemental material). To investigate the cap-binding activity of the polymerases, UV cross-linking assays were carried out (Fig. 1B). Cap1-RNA specifically bound to PB2 in both the FluA and FluB polymerases, although the cap-binding activity of FluB PB2 is less (~25%) than that of FluA PB2. These results suggest that the FluA and FluB polymerases are different in their binding to RNA containing the cap1 structure and in their cleavage modes.

Specificity of recognition of cap structures by Flu polymerases. To investigate the specificity of recognition of cap structures by FluA and FluB polymerases, we carried out similar experiments using RNA primers containing various cap structures. To this end, we prepared ^{32}P-labeled RNAs containing differently methylated cap structures, such as $m^7GpppGm$, m^7GpppG, and GpppG, as described in Materials and Methods. After preparation, we analyzed the terminal cap structure using nuclease-digested samples (see Materials and Methods) and thin-layer chromatography on a PEI-cellulose plate. As shown in Fig. 2A, we confirmed that each RNA

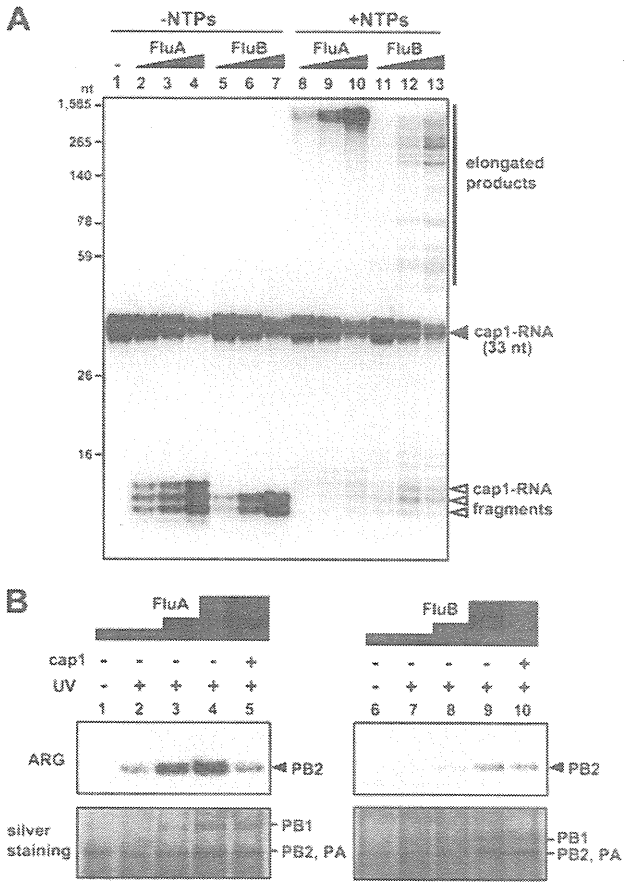

FIG. 1. *In vitro* capped RNA cleavage, RNA elongation and cap-binding reactions. (A) Dose dependency of *in vitro* capped RNA cleavage and subsequent RNA elongation by vRNP. *In vitro* capped RNA cleavage and RNA elongation reactions were performed with 20, 40, and 80 ng of FluA (lanes 2 to 4 and 8 to 10) and FluB (lanes 5 to 7 and 11 to 13) vRNP using 2 fmol of m^7GpppGm-RNA. Capped RNA cleavage was performed in the absence of NTPs (lanes 2 to 7), while RNA elongation was performed in the presence of NTPs (lanes 8 to 13). Synthesized RNA products were analyzed by 15% PAGE containing 8 M urea. (B) Interaction of vRNP with the cap1 structure. UV cross-linking was performed using 50, 100, and 200 ng of FluA (lanes 1 to 5) and FluB (lanes 6 to 10) vRNPs with (lanes 2 to 5 and 7 to 10) or without (lanes 1 and 6) UV irradiation at 254 nm. Competition experiments were performed in the presence of 100 pmol of m^7GpppGm analogue (lanes 5 and 10). Upper panels show autoradiography (ARG), while lower panels show silver staining patterns.

had the expected cap structure. Using these RNAs as substrates, we carried out *in vitro* capped RNA cleavage and subsequent RNA elongation reactions with FluA or FluB vRNPs. As expected, FluA vRNP specifically cleaved both m^7GpppGm-RNA and m^7GpppG-RNA, although the latter was less efficiently cleaved (Fig. 2B, lanes 2, 5, and 8, and D). The m^7GpppGm-RNA fragments were most successfully elongated into viral mRNAs (Fig. 2C, lane 2, and E). In contrast, FluB vRNP could cleave GpppG-RNA efficiently in addition to the m^7GpppGm-RNA and m^7GpppG-RNA (Fig. 2B, lanes 3, 6, and 9, and D). It is noteworthy that m^7GpppGm-RNA fragments also served as an efficient primer for chain elongation, as is the case for the FluA polymerase (Fig. 2C, lane 3, and E). Moreover, we carried out UV cross-linking assays using RNA primers containing various cap structures (Fig. 2F). Interestingly, the cap-binding activity was detected just using m^7GpppGm-RNA with both FluA and FluB vRNPs. These results indicate that the guanine-7-methyl residue is a key for stable cap binding of both FluA and FluB polymerases. It is also indicated that the cap-binding activity is strictly related to the elongation efficiency but not to the cleavage reaction. It is presently unknown why the binding of GpppG and m^7GpppG was not detected under the conditions employed, while m^7GpppG-RNA was recognized and cleaved by both FluA and FluB polymerases and GpppG-RNA was by the FluB polymerase. Since m^7GpppG-RNA and GpppG-RNA were not effective for elongation, the cleavage of these cap structures would be abortive for transcription, possibly due to improper recognition.

Identification of key amino acids involved in the cap recognition specificity of the PB2 subunit of the FluB polymerase. To clarify the cap recognition mechanism, we focused our structure-related functional studies on the interaction between the cap1 structure and the PB2 subunit, which has the cap-binding domain. It is quite likely that amino acid residues essential for cap binding are conserved between FluA and FluB (Fig. 3A). Three-dimensional (3D) structural studies (12) revealed that in the FluA PB2 cap-binding domain (Fig. 3B), Phe404 and His357 sandwich the methylated guanine and Phe323 stacks on the ribose of m^7GTP. Glu361 makes hydrogen bonds with the N1 and N2 positions of guanine, and Lys376 also makes a hydrogen bond with position O6 of guanine. Computer-associated modeling could make the FluB PB2 cap-binding domain fit on the FluA PB2 cap-binding domain (Fig. 3C). In the model of the FluB cap-binding domain, 2 amino acids, Gln325 and Trp359, are different from Phe323 and His357 of the FluA cap-binding domain, respectively.

To determine key amino acids related to the cap recognition specificity, the transcription activity was measured using a minireplicon assay system. In this assay system, we have used a transient-transfection system with a viral genome, in which the coding region for a viral gene is replaced with a luciferase reporter gene while *cis*-acting regulatory regions (24) remain intact (35). The cellular RNA polymerase I produces a negative-sense luciferase RNA sandwiched with viral terminal sequences. Luciferase mRNA is synthesized by transcription of the negative-sense RNA with the viral RNA polymerase and NP and subjected to translation. This system has been used to measure the transcription activity of the Flu polymerase (20, 22).

In the case of FluA PB2, His357, with which methylated guanine is stacked, could be replaced by other aromatic residues such as Trp and Phe, while Phe404, which is also involved in stacking methylated guanine, could not be (Fig. 4A). Leu could not substitute for either His357 and Phe404. On the other hand, in the case of FluB PB2, Trp359 could be replaced with other aromatic residues (but with less efficiency than for the FluA polymerase), but Phe406 could be replaced with hydrophobic residues such as Tyr and Leu (Fig. 4B). To confirm the importance of the hydrogen bonds with methylated guanine, Glu361 and Lys376 in FluA PB2 and Glu363 and Lys378 in FluB PB2 were replaced with alanine (Ala). Ala substitutions in FluA PB2 abolished the transcription activity,

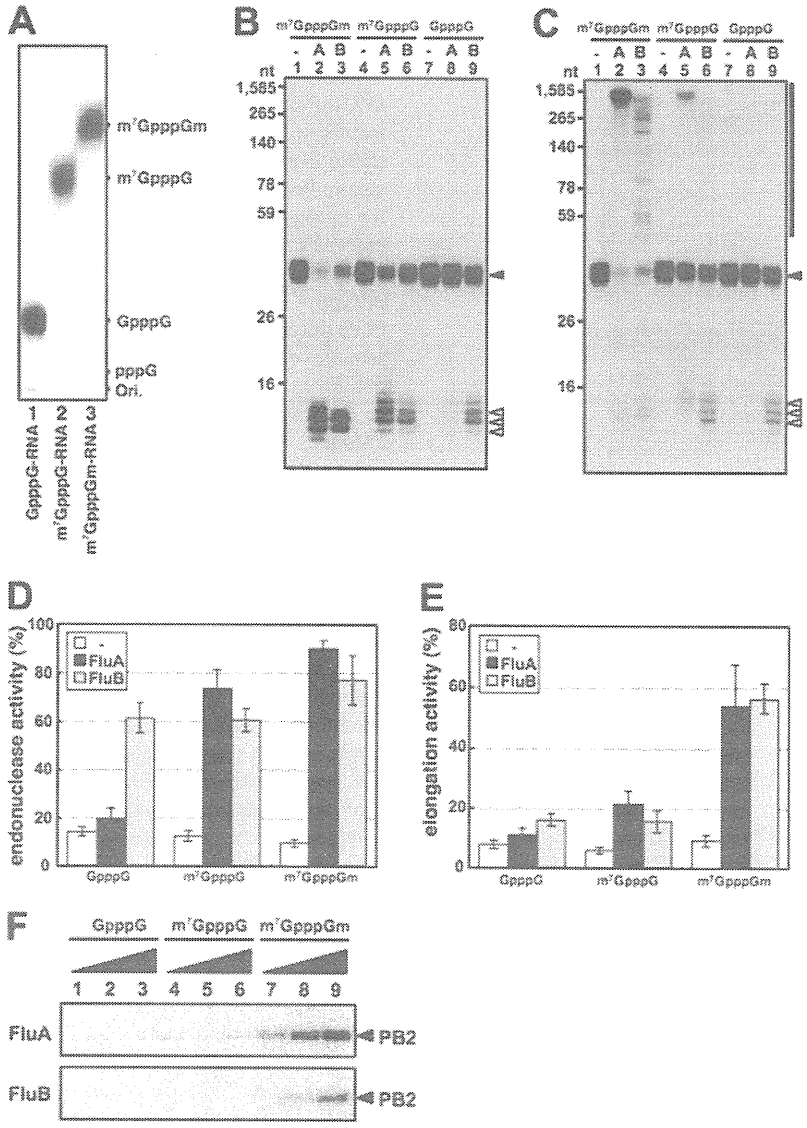

FIG. 2. Specificity of recognition of cap structures by Flu polymerases. (A) Analysis of 5′-terminal cap structures of RNAs. T7 RNA polymerase-synthesized RNAs were treated with nuclease P_1 and analyzed by TLC (PEI-CEL, 0.65 M LiCl), and radioactive nucleotides were detected by autoradiography. (B and C) *In vitro* capped RNA cleavage (B) and RNA elongation (C) reactions were performed with 600 ng of FluA (lanes 2, 5, and 8) or FluB (lanes 3, 6, and 9) vRNP using 2 fmol of variously methylated capped RNAs (m^7GpppGm-RNA, lanes 1 to 3; m^7GpppG-RNA, lanes 4 to 6; GpppG-RNA, lanes 7 to 9). RNA products were analyzed by 15% PAGE containing 8 M urea. The input capped RNAs (33 nt), the cleaved capped RNA products, and the elongated products are indicated as a closed triangle, open triangles, and a black bar, respectively, at the right. (D and E) Ratios of cleaved RNA products (D) and RNA transcripts (E) to total input primer RNAs. (F) Cap-binding activity for variously methylated capped RNAs. UV cross-linking was performed using 50, 100, and 200 ng of FluA (upper panel) and FluB (lower panel) vRNP and 50 fmol of variously methylated capped RNAs (GpppG-RNA, lanes 1 to 3; m^7GpppG-RNA, lanes 4 to 6; m^7GpppGm-RNA, lanes 7 to 9).

while Ala substitution for Lys378 of FluB PB2 caused only a small decrease in the transcription activity (Fig. 4C and D). These results suggest that the stacking interaction of His357 and Phe404 and the hydrogen bonds of Glu361 and Lys376 with methylated guanine are essential for cap recognition by the FluA polymerase. This is in good agreement with a previous report (12). In contrast, it is suggested that the stacking interaction of Trp359 and the hydrogen bonds of Glu363 with methylated guanine are sufficient for cap recognition by the FluB polymerase. These results indicate that the mechanism for recognition of methylated guanine by the FluB polymerase could be different from that for the FluA polymerase. It is also speculated that the cap-binding pocket of the FluB polymerase may be more flexible or less stringent than that of the FluA polymerase in recognition of various cap structures, since Phe406 of FluB PB2 is changeable with other amino acids.

Phe323 in FluA PB2 stacks on the ribose of m^7GTP and was essential for cap recognition (see Fig. S3 in the supplemental

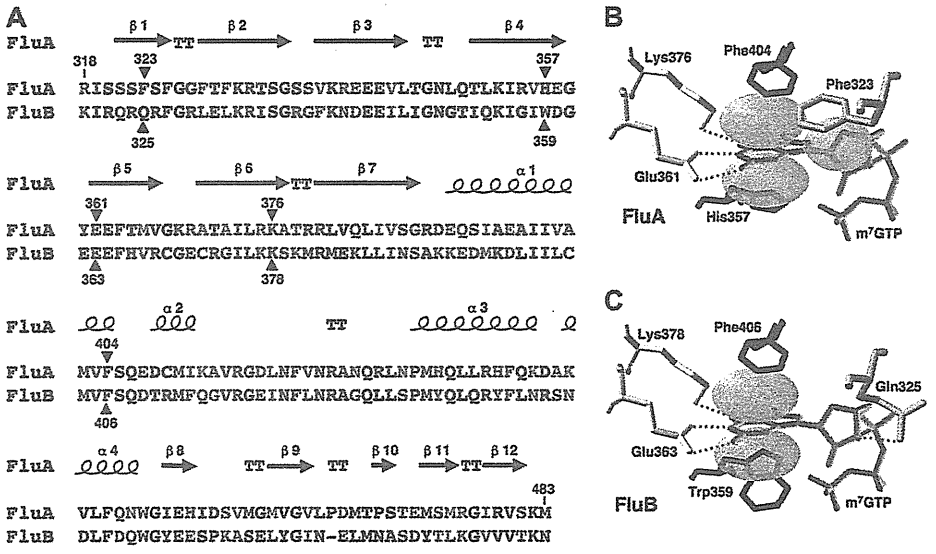

FIG. 3. Structure of the PB2 cap-binding domain. (A) Sequence alignment of the PB2 cap-binding domains of FluA (A/Panama/2007/99) and FluB (B/Shanghai/361/2002). The secondary structure of FluA is displayed over the sequence alignment. Blue letters and green letters show identical residues and similar residues, respectively. Purple triangles indicate the residues in contact with the cap analogue m^7GTP. (B and C) Model of m^7GTP interaction with the cap-binding domains of FluA PB2 (B) (10) and FluB PB2 (C) drawn by computer-associated calculation, with putative hydrogen bonds shown as green dotted lines.

material) (12). However, it is likely that Gln325 in FluB PB2, which is located in the same position of Phe323 in FluA PB2, makes a hydrogen bond with the ribose of m^7GTP. We speculated that FluB PB2 recognizes the cap structure in a flexible pocket as discussed above, so that the hydrogen bonds made by Gln325 and Glu363 could be more crucial for cap binding than those in FluA PB2. In addition, there could be an appropriate amino acid in the amino acid combination between amino acid positions 325 and 363 in FluB PB2 in order to keep the flexible pocket. To confirm this prediction, the transcription activities of mutants with substitutions at position 325 were examined in the presence of the Asp363 mutant (Fig. 4E). The transcription activity of the Asp363 single mutant was reduced to 20% of the wild-type level, possibly because of a longer distance between Asp363 and guanine residues for hydrogen bonds (Fig. 4E; see Fig. S4B in the supplemental material). Interestingly, Lys and Arg mutations but not Ala and Asn mutations at position 325 could rescue the transcription activity of Asp363 (Fig. 4E). We also examined the effect of an Asp363 single mutation and an Arg325-Asp363 double mutation on the transcription and replication processes and the cap-binding activity (Fig. 5). According to the levels of accumulation of mRNA (Fig. 5A) and cRNA (Fig. 5B), the level of reporter expression (Fig. 4E) is well correlated with the transcription but not the replication activities. To examine the cap-binding activity *in vivo*, capped RNAs that could interact with the viral RNA polymerase were coprecipitated from cells expressing the recombinant RNA polymerase, and the cap structure was detected by recapping of RNA which had been CIAP treated and then decapped (β-eliminated) (Fig. 5C). We could detect the [^{32}P]m^7Gp labeled by [α-^{32}P]GTP and vaccinia virus capping enzyme, depending on TAP digestion. In contrast, uncapped RNA treated with CIAP was poorly labeled by this protocol. These results indicate that this recapping method is suitable for the detection of capped RNA specifically. Using this method, we found that the cap-binding activities of these mutants (Fig. 5D) are well correlated with these transcription activities (Fig. 4E) and the mRNA accumulation levels (Fig. 5A). These results indicate that the Arg at position 325 in FluB PB2 supports cap recognition when Glu363 is replaced with Asp363.

DISCUSSION

Most of our knowledge on the transcription mechanism of the influenza virus genome has been derived from studies on FluA, while little has been demonstrated for FluB. This is also the case for studies on the enzymatic aspects of these viral RNA polymerases. Each of the two methyl groups in the cap1 structure, the 7-methyl residue of the guanine base and the 2′-*O*-methyl residue on the ribose of the penultimate base, strongly influences the transcription activity of the FluA polymerase (4). Recently, the structure of the PB2 cap-binding domain of the FluA polymerase with m^7GTP has been clarified (12). Based on these reports, we tried to identify the specificity of cap recognition and characterize key amino acids for cap recognition of the FluB polymerase.

First, we compared the efficiencies of capped RNA cleavage and subsequent RNA elongation reactions of the FluA polymerase with those of the FluB polymerase using cap1-RNA. As expected, the FluA polymerase exhibited efficient endonuclease activity, elongation activity, and cap-binding affinity. The pattern of cleavage of cap1-RNA by the FluB polymerase was different from that by the FluA polymerase (Fig. 1A; see Fig. S1B in the supplemental material), and the RNA elongation and cap-binding activities of the FluB polymerase were lower than those of the FluA polymerase (Fig. 1A and B). These results indicate that the cap binding and cleavage mechanism

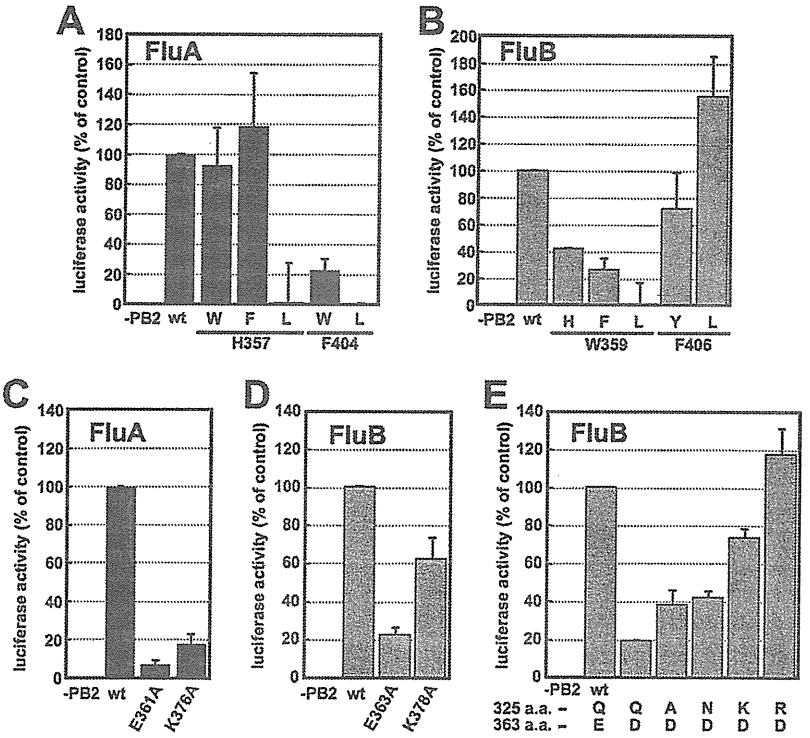

FIG. 4. Transcription activities of PB2 mutants in a minireplicon system. (A and B) Effects of mutations of m^7GTP stacking residues in FluA (A) and FluB (B) PB2 on transcription activity. (C and D) Effects of mutations in residues involved in hydrogen bonds with the guanine residue of m^7GTP in FluA (C) and FluB (D) PB2 on transcription activity. (E) Effect of mutations in Gln325 with an Asp mutation at position 363 in FluB PB2 on transcription activity. The firefly luciferase activity was normalized to *Renilla* luciferase activity. The results are averages and standard deviations (SD) from four independent experiments.

of the FluB polymerase are different from those of the FluA polymerase.

We then examined the specificity of recognition of cap structures by the FluB polymerase compared with that by the FluA polymerase. Using various methylated capped RNAs, we performed capped RNA cleavage and RNA elongation assays (Fig. 2). The FluA polymerase cleaved RNA containing m^7G specifically, while the FluB polymerase could cleave GpppG-RNA as well as RNA containing m^7G. Both the FluA and FluB polymerases elongated and bound to the cap structure efficiently only in the case of $m^7GpppGm$-RNA compared with other capped RNAs (Fig. 2C, 2E, and 2F). Based on these results, we propose that the FluA polymerase recognizes strictly the guanine-7-methyl residue in the cleavage reaction and that the FluB polymerase recognizes only the cap core structure (GpppX), which may result in its weak cap1-binding activity. In addition, these results suggest that the ribose 2′-*O*-methyl residue and/or the guanine-7-methyl residue may be responsible for the elongation reaction by both FluA and FluB polymerases, because cap binding and efficient elongation could not be observed except for $m^7GpppGm$-RNA.

To elucidate the mechanism of cap recognition by the FluB polymerase, we studied the PB2 subunit, which has the cap-binding domain. Recently, the 3D structure of the FluA PB2 cap-binding domain was revealed (12). Amino acid residues essential for cap binding were identified and found to be conserved between FluA and FluB polymerases (Fig. 3A). In the FluA PB2 cap-binding domain (Fig. 3B), the methylated guanine base is sandwiched with His357 and Phe404, and Phe323 stacks on the ribose of m^7GTP. Glu361 makes hydrogen bonds with the N1 and N2 positions of guanine, and Lys376 also makes hydrogen bonds with the O6 position of guanine. Based on the structure of the FluA PB2 cap-binding domain, a model of the FluB PB2 cap-binding domain was postulated (Fig. 3C). Five amino acids which contact the guanine-7-methyl residue are highlighted. Minireplicon assays showed that Trp359 in FluB PB2 is crucial for possible stacking interaction with a methylated guanine base without sandwiching with Phe406 (Fig. 4B). Moreover, the hydrogen bond made by Lys378 to the O6 position of guanine seemed not to be essential for cap recognition (Fig. 4D). These results suggest that the FluB polymerase recognizes the cap structure in a manner different from the FluA polymerase. We illustrated a new proposed computer-associated model for cap recognition by FluB PB2 (see Fig. S4A in the supplemental material), although the 3D structure of the FluB PB2 cap-binding domain has not been determined. The overall structures of four cap-binding proteins, FluA PB2 (12), eIF4E (33, 34), CBP20 (23), and VP39 (16), differ each other widely due to their evolutionarily unrelated origins, but the cap-binding pockets are essentially quite similar (see Fig. S5 in the supplemental material), although there are some differences in details. In addition to the two aromatic amino acids, an acidic residue is directed toward the pocket to accommodate the positively charged π-ring system of

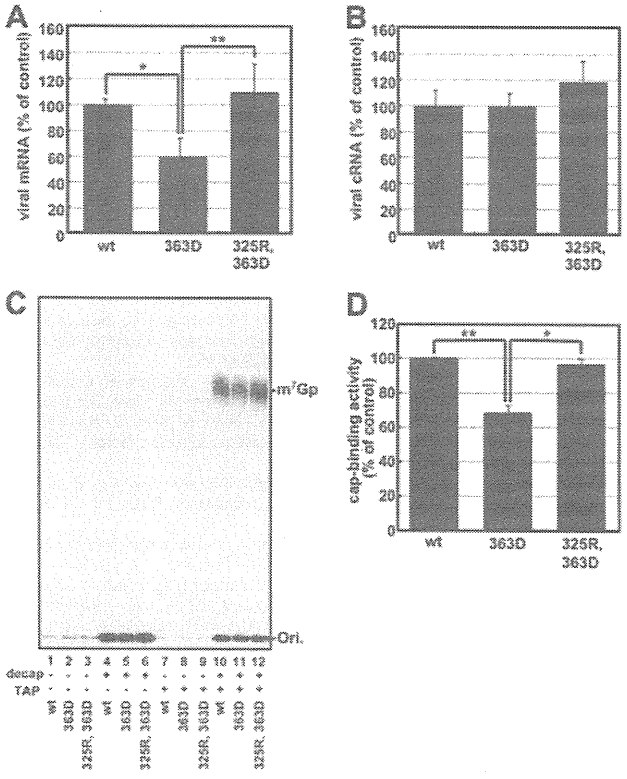

FIG. 5. Suppression mutation in transcription and cap-binding activities for the FluB PB2-363D mutant. (A and B) The levels of accumulation of viral mRNA (A) and cRNA (B) were measured by qPCR. (C) Cap-binding activities of mutants. Coprecipitated capped RNAs with 100 ng of recombinant RNA polymerase complexes (wild type [wt], lanes 1, 4, 7, and 10; 363D mutant, lanes 2, 5, 8, and 11; 325R-363D double mutant, lanes 3, 6, 9, and 12) were recapped before (lanes 1 to 3 and 7 to 9) and after (lanes 4 to 6 and 10 to 12) decapping by β-elimination. Recapped RNAs were treated without (lanes 1 to 6) or with (lanes 7 to 12) tobacco acid pyrophosphatase (TAP) and analyzed by TLC (PEI-CEL, 0.65 M LiCl), and radioactive nucleotides were determined by autoradiography. (D) The radioactivity of [^{32}P]m^{7}Gp of TAP-treated products which were recapped after decapping was counted with a liquid scintillation counter. The cap-binding activity is represented as a ratio to the amount of [^{32}P]m^{7}Gp derived from the wild type. These results are averages and SD from three independent experiments, and the level of significance was determined by Student's *t* test (unpaired) (*, $P < 0.0025$; **, $P < 0.0005$).

the methylated guanine. These amino acids provide high specificity for the recognition of m^{7}GTP and exhibit low affinity for nonmethylated cap analogues (>100-fold difference in affinity compared with N^7-methylated ones) (15, 18, 26). Compared with these well-known cap-binding proteins, the cap-binding pocket of FluB PB2 contains only one aromatic amino acid, Trp359. This feature may cause the low affinity of FluB PB2 for the cap1 structure (Fig. 1B) and the recognition of nonmethylated capped RNA (GpppG-RNA) (Fig. 2) compared with FluA PB2.

In the case of FluA PB2, the stacking interaction of Phe323 with the ribose of m^{7}GTP is also essential for cap recognition. However, Gln325 of FluB PB2 seems to make a hydrogen bond with the ribose of m^{7}GTP instead of a stacking interaction. To examine our speculation that FluB PB2 recognizes the cap structure in the flexible pocket, we made substitution mutations at position 325 in the presence of an Asp363 mutation (Gln → Asp), which should extend too much into the pocket where Gln325 is present. Interestingly, the transcription activity and the cap-binding activity of the Asp363 mutant were restored to the wild-type levels by the Arg325 mutation (Fig. 4E and 5) without changing the replication activity. The transcription activity of the Asp363 single mutant was decreased, possibly because the longer distance between Asp363 and the guanine residue may make hydrogen bonds weak (see Fig. S4B in the supplemental material). These results suggest that the hydrogen bond made by Arg325 with the ribose of the guanosine could support the recognition of the cap structure (Fig. 4E, 5A, 5C, and 5D; see Fig. S4C in the supplemental material). Crystal structure analyses of wild-type FluB PB2 and the mutant containing Arg325 and Asp363 are needed to support our hypothesis.

In summary, our results indicate that the substrate specificity and the residues essential in the cap recognition are different between FluA and FluB polymerases. In the case of the FluA polymerase, m^{7}G-capped RNA is cleaved specifically, and the stacking interactions of His357 and Phe404 with the methylated guanine base and of Phe323 with the ribose of m^{7}GTP and the hydrogen bonds made by Glu361 and Lys376 on the methylated guanine are essential for cap recognition as observed in other cap-binding proteins. In contrast, in the case of the FluB polymerase, unmethylated capped RNA is cleaved as well as m^{7}G-capped RNA, and the stacking interaction which is made only by Trp359 with the guanine base and the hydrogen bonds which are made by Glu363 on the guanine base and by Gln325 with the ribose of m^{7}GTP are enough for cap recognition.

ACKNOWLEDGMENTS

We thank Y. Suzuki and T. Gotanda (Kitasato Institute, Research Center for Biologicals, Saitama, Japan) for providing the purified influenza virus A/Panama/2007/99 and B/Shanghai/361/02 virions. We also thank T. Ogino (Lemer Research Institute, Cleveland Clinic, Cleveland, OH) and A. Kawaguchi (Kitasato Institute for Life Sciences, Kitasato University, Tokyo, Japan) for critical discussion.

This research was supported in part by a grant-in-aid from the Ministry of Education, Culture, Sports, Science, and Technology of Japan (to K.N.).

REFERENCES

1. **Argos, P.** 1988. A sequence motif in many polymerases. Nucleic Acids Res. **16:**9909–9916.
2. **Biswas, S. K., P. L. Boutz, and D. P. Nayak.** 1998. Influenza virus nucleoprotein interacts with influenza virus polymerase proteins. J. Virol. **72:**5493–5501.
3. **Bouloy, M., M. A. Morgan, A. J. Shatkin, and R. M. Krug.** 1979. Cap and internal nucleotides of reovirus mRNA primers are incorporated into influenza viral complementary RNA during transcription in vitro. J. Virol. **32:**895–904.
4. **Bouloy, M., S. J. Plotch, and R. M. Krug.** 1980. Both the 7-methyl and the 2′-O-methyl groups in the cap of mRNA strongly influence its ability to act as primer for influenza virus RNA transcription. Proc. Natl. Acad. Sci. U. S. A. **77:**3952–3956.
5. **Bouloy, M., S. J. Plotch, and R. M. Krug.** 1978. Globin mRNAs are primers for the transcription of influenza viral RNA in vitro. Proc. Natl. Acad. Sci. U. S. A. **75:**4886–4890.
6. **Braam, J., I. Ulmanen, and R. M. Krug.** 1983. Molecular model of a eucaryotic transcription complex: functions and movements of influenza P proteins during capped RNA-primed transcription. Cell **34:**609–618.
7. **Chen, Z., et al.** 1998. Comparison of the ability of viral protein-expressing plasmid DNAs to protect against influenza. Vaccine **16:**1544–1549.
8. **Dias, A., et al.** 2009. The cap-snatching endonuclease of influenza virus polymerase resides in the PA subunit. Nature **458:**914–918.

9. **Engelhardt, O. G., and E. Fodor.** 2006. Functional association between viral and cellular transcription during influenza virus infection. Rev. Med. Virol. **16:**329–345.
10. **Fodor, E., et al.** 2002. A single amino acid mutation in the PA subunit of the influenza virus RNA polymerase inhibits endonucleolytic cleavage of capped RNAs. J. Virol. **76:**8989–9001.
11. **Fraenkel-Conrat, H., and A. Steinschneider.** 1967. Stepwise degradation of RNA: periodate followed by aniline cleavage. Methods Enzymol. **12B:**243–246.
12. **Guilligay, D., et al.** 2008. The structural basis for cap binding by influenza virus polymerase subunit PB2. Nat. Struct. Mol. Biol. **15:**500–506.
13. **Hara, K., F. I. Schmidt, M. Crow, and G. G. Brownlee.** 2006. Amino acid residues in the N-terminal region of the PA subunit of influenza A virus RNA polymerase play a critical role in protein stability, endonuclease activity, cap binding, and virion RNA promoter binding. J. Virol. **80:**7789–7798.
14. **He, X., et al.** 2008. Crystal structure of the polymerase PA(C)-PB1(N) complex from an avian influenza H5N1 virus. Nature **454:**1123–1126.
15. **Hodel, A. E., P. D. Gershon, X. Shi, S. M. Wang, and F. A. Quiocho.** 1997. Specific protein recognition of an mRNA cap through its alkylated base. Nat. Struct. Biol. **4:**350–354.
16. **Hu, G., P. D. Gershon, A. E. Hodel, and F. A. Quiocho.** 1999. mRNA cap recognition: dominant role of enhanced stacking interactions between methylated bases and protein aromatic side chains. Proc. Natl. Acad. Sci. U. S. A. **96:**7149–7154.
17. **Iwatsuki-Horimoto, K., et al.** 2008. Limited compatibility between the RNA polymerase components of influenza virus type A and B. Virus Res. **135:**161–165.
18. **Izaurralde, E., J. Stepinski, E. Darzynkiewicz, and I. W. Mattaj.** 1992. A cap binding protein that may mediate nuclear export of RNA polymerase II-transcribed RNAs. J. Cell Biol. **118:**1287–1295.
19. **Kawaguchi, A., T. Naito, and K. Nagata.** 2005. Involvement of influenza virus PA subunit in assembly of functional RNA polymerase complexes. J. Virol. **79:**732–744.
20. **Labadie, K., E. Dos Santos Afonso, M. A. Rameix-Welti, S. van der Werf, and N. Naffakh.** 2007. Host-range determinants on the PB2 protein of influenza A viruses control the interaction between the viral polymerase and nucleoprotein in human cells. Virology **362:**271–282.
21. **Lamb, R. A., and P. W. Choppin.** 1977. Synthesis of influenza virus polypeptides in cells resistant to alpha-amanitin: evidence for the involvement of cellular RNA polymerase II in virus replication. J. Virol. **23:**816–819.
22. **Li, C., M. Hatta, S. Watanabe, G. Neumann, and Y. Kawaoka.** 2008. Compatibility among polymerase subunit proteins is a restricting factor in reassortment between equine H7N7 and human H3N2 influenza viruses. J. Virol. **82:**11880–11888.
23. **Mazza, C., A. Segref, I. W. Mattaj, and S. Cusack.** 2002. Large-scale induced fit recognition of an m(7)GpppG cap analogue by the human nuclear cap-binding complex. EMBO J. **21:**5548–5557.
24. **Neumann, G., et al.** 1999. Generation of influenza A viruses entirely from cloned cDNAs. Proc. Natl. Acad. Sci. U. S. A. **96:**9345–9350.
25. **Neumann, G., A. Zobel, and G. Hobom.** 1994. RNA polymerase I-mediated expression of influenza viral RNA molecules. Virology **202:**477–479.
26. **Niedzwiecka, A., et al.** 2002. Biophysical studies of eIF4E cap-binding protein: recognition of mRNA 5′ cap structure and synthetic fragments of eIF4G and 4E-BP1 proteins. J. Mol. Biol. **319:**615–635.
27. **Obayashi, E., et al.** 2008. The structural basis for an essential subunit interaction in influenza virus RNA polymerase. Nature **454:**1127–1131.
28. **Ogino, T., M. Kobayashi, M. Iwama, and K. Mizumoto.** 2005. Sendai virus RNA-dependent RNA polymerase L protein catalyzes cap methylation of virus-specific mRNA. J. Biol. Chem. **280:**4429–4435.
29. **Plotch, S. J., J. Tomasz, and R. M. Krug.** 1978. Absence of detectable capping and methylating enzymes in influenza virions. J. Virol. **28:**75–83.
30. **Shimizu, K., H. Handa, S. Nakada, and K. Nagata.** 1994. Regulation of influenza virus RNA polymerase activity by cellular and viral factors. Nucleic Acids Res. **22:**5047–5053.
31. **Sugiyama, K., et al.** 2009. Structural insight into the essential PB1-PB2 subunit contact of the influenza virus RNA polymerase. EMBO J. **28:**1803–1811.
32. **Tomassini, J. E.** 1996. Expression, purification, and characterization of orthomyxovirus: influenza transcriptase. Methods Enzymol. **275:**90–99.
33. **Tomoo, K., et al.** 2002. Crystal structures of 7-methylguanosine 5′-triphosphate (m(7)GTP)- and P(1)-7-methylguanosine-P(3)-adenosine-5′,5′-triphosphate (m(7)GpppA)-bound human full-length eukaryotic initiation factor 4E: biological importance of the C-terminal flexible region. Biochem. J. **362:**539–544.
34. **Tomoo, K., et al.** 2003. Structural features of human initiation factor 4E, studied by X-ray crystal analyses and molecular dynamics simulations. J. Mol. Biol. **328:**365–383.
35. **Turan, K., et al.** 2004. Nuclear MxA proteins form a complex with influenza virus NP and inhibit the transcription of the engineered influenza virus genome. Nucleic Acids Res. **32:**643–652.
36. **Yuan, P., et al.** 2009. Crystal structure of an avian influenza polymerase PA(N) reveals an endonuclease active site. Nature **458:**909–913.

JOURNAL OF VIROLOGY, July 2011, p. 6197–6204 Vol. 85, No. 13
0022-538X/11/$12.00 doi:10.1128/JVI.00277-11

Replication-Coupled and Host Factor-Mediated Encapsidation of the Influenza Virus Genome by Viral Nucleoprotein▽

Atsushi Kawaguchi,[1,2] Fumitaka Momose,[2] and Kyosuke Nagata[1]*

Department of Infection Biology, Graduate School of Comprehensive Human Sciences, University of Tsukuba, 1-1-1 Tennodai, Tsukuba 305-8575, Japan,[1] and Kitasato Institute for Life Sciences, Kitasato University, 5-9-1 Shirokane, Minato-ku, Tokyo 108-8641, Japan[2]

Received 7 February 2011/Accepted 11 April 2011

The influenza virus RNA-dependent RNA polymerase is capable of initiating replication but mainly catalyzes abortive RNA synthesis in the absence of viral and host regulatory factors. Previously, we reported that IREF-1/minichromosome maintenance (MCM) complex stimulates a *de novo* initiated replication reaction by stabilizing an initiated replication complex through scaffolding between the viral polymerase and nascent cRNA to which MCM binds. In addition, several lines of genetic and biochemical evidence suggest that viral nucleoprotein (NP) is involved in successful replication. Here, using cell-free systems, we have shown the precise stimulatory mechanism of virus genome replication by NP. Stepwise cell-free replication reactions revealed that exogenously added NP free of RNA activates the viral polymerase during promoter escape while it is incapable of encapsidating the nascent cRNA. However, we found that a previously identified cellular protein, RAF-2p48/NPI-5/UAP56, facilitates replication reaction-coupled encapsidation as an NP molecular chaperone. These findings demonstrate that replication of the virus genome is followed by its encapsidation by NP in collaboration with its chaperone.

The genome of influenza type A viruses consists of eight-segmented and single-stranded RNAs of negative polarity. Transcription from the viral RNA (vRNA) genome is initiated using the oligonucleotide containing the cap-1 structure from cellular pre-mRNAs as a primer, whereas genome replication is primer independent and generates full-length vRNA through cRNA (full-sized complementary copy of vRNA) (reviewed in reference 17). Generally, each viral DNA or RNA genome is not present as a naked form but as a complex with viral basic proteins. The influenza virus genome exists as a ribonucleoprotein (termed vRNP) complex with nucleoprotein (NP), one of the basic viral proteins, and viral RNA-dependent RNA polymerases consisting of three subunits (PB1, PB2, and PA). NP binds single-stranded RNA without sequence specificity and is required for maintaining the RNA template in an ordered conformation suitable for viral RNA synthesis and packaging into virions (6, 23, 34). In the case of *Mononegavirales*, nonsegmented and negative-stranded RNA viruses, it is proposed that the nucleocapsid (N) protein forms a trimeric complex with the viral RNA polymerase large (L) protein and phosphoprotein (P) to form a replicase complex to produce the progeny viral genome with concomitant encapsidation of nascent RNA by N protein and that encapsidation is mediated by the chaperone activity of P protein (2, 7, 14, 24). In the case of influenza virus, it is also postulated that NP might regulate the viral polymerase function and encapsidate the virus genome through its interaction with PB1 and/or PB2 (1, 23). Genetic analyses suggest that NP participates in the replication process (15). Recently, it was also shown that NP that is saturated with single-stranded DNA (ssDNA), resulting in the lack of RNA binding activity, stimulates virus genome replication from a model template without primer (18). It is possible that NP stimulates virus genome replication through interaction with the viral polymerase in an RNA binding activity-independent manner. Moreover, the *in vitro* cRNA synthesis using infected cell extracts as an enzyme source depends on a supply of NP free of RNA (27). This finding has been interpreted as indicating that NP prevents the premature termination of RNA synthesis, possibly by binding to nascent RNA chains, that is, encapsidating them. Based on these observations, it could be hypothesized that NP facilitates virus genome replication by both RNA binding- and viral polymerase binding-dependent mechanisms. It is proposed that encapsidation is initiated by successive targeting of exogenous NP monomer to a replicating RNA through the interaction between NP and the viral polymerase, which is distinct from the replicative enzyme bound to the 5′ end of nascent RNA (1, 8, 11, 22), and then additional NP molecules are subsequently recruited by the NP-NP oligomerization (3, 23). It is also reported that nascent cRNA is degraded by host cellular nucleases unless it is stabilized by newly synthesized viral RNA polymerases and NP (33). However, the precise molecular mechanisms involved in virus genome replication and encapsidation by NP are yet unclear.

The cRNA synthesis occurs from incoming vRNA in infected cells, but vRNP complexes isolated from virions by themselves hardly synthesize cRNA (9). Thus, it was reasonable to examine whether a host factor(s) and/or a viral factor(s) is required for the replication process. We reconstituted a cell-free virus genome replication system with virion-associated vRNP and nuclear extracts prepared from uninfected HeLa cells (9). Using biochemical fractionation and complementation assays, we identified influenza virus replication factor 1 (IREF-1) that enabled the viral polymerase to synthesize

* Corresponding author. Mailing address: Department of Infection Biology, Graduate School of Comprehensive Human Sciences, University of Tsukuba, 1-1-1 Tennodai, Tsukuba 305-8575, Japan. Phone and fax: 81 29 853 3233. E-mail: knagata@md.tsukuba.ac.jp.

▽ Published ahead of print on 20 April 2011.

full-sized cRNA. Otherwise, the viral RNA polymerase produces mainly abortive short RNA chains in the absence of IREF-1. IREF-1 was found to be identical with a minichromosome maintenance (MCM) heterohexamer complex. IREF-1/MCM stabilizes replicating polymerase complexes by promoting the interaction between the nascent cRNA and the PA subunit.

Here, we examined the molecular function of NP in influenza virus genome replication using a previously established cell-free virus genome replication system and virion-associated vRNP. Exogenously added NP free of RNA stimulated virus genome replication with MCM in an additive manner. Further, we found that NP activates the viral polymerase during its transition from initiation to elongation to synthesize the unprimed full-length cRNA, but NP by itself is incapable of encapsidating the nascent cRNA. However, we found that RAF-2p48/NPI-5/UAP56/BAT1, which was identified as a host factor for activation of viral RNA synthesis (16), is required for the encapsidation of nascent cRNA with exogenously added NP free of RNA and for the stimulation of the elongation process of virus genome replication. We observed that the level of the virus genome replication was decreased in infected cells when the expression of the RAF-2p48/UAP56 gene was knocked down by small interfering RNA (siRNA)-mediated gene silencing. Based on these observations, we propose an NP- and host factor-dependent mechanism of virus genome encapsidation in concert with its replication.

MATERIALS AND METHODS

Biological materials. vRNP was prepared from purified influenza A/Puerto Rico/8/34 virus as previously described (28). For the expression of His-tagged NP (His-NP), we cloned the open reading frame (ORF) corresponding to the NP gene into pET14b. Rabbit polyclonal antibody against NP was generated by immunization of a 2-month-old female rabbit with His-NP protein. HeLa cells were grown in Dulbecco's modified Eagle's medium (DMEM) supplemented with 10% fetal bovine serum.

Preparation of recombinant proteins. His-tagged recombinant proteins were prepared and purified according to the manufacturer's protocol. In addition, to remove the bacterial RNA possibly bound to NP, we treated recombinant proteins with RNase A before purification and washed them with a buffer containing 1 M NaCl. Recombinant RAF-2p48/UAP56 was prepared from glutathione *S*-transferase (GST)-tagged RAF-2p48/UAP56 by PreScission protease (GE Health Care) digestion. Purified proteins were stored in a buffer containing 50 mM HEPES-NaOH (pH 7.9), 300 mM KCl, 20% glycerol, and 1 mM dithiothreitol (DTT) at −80°C until use. Recombinant MCM complex was prepared as previously described (9). These purified recombinant proteins were separated by SDS-PAGE and visualized by staining with Coomassie brilliant blue in Fig. 1A.

Cell-free virus genome replication system. Cell-free virus genome replication was carried out at 30°C for 90 min in a final volume of 25 μl containing 50 mM HEPES-NaOH (pH 7.9), 5 mM $MgCl_2$, 50 mM KCl, 1.5 mM dithiothreitol, 500 μM each ATP, CTP, and UTP, 25 μM GTP, 5 μCi of [α-^{32}P]GTP (3,000 Ci/mmol), 8 U of RNase inhibitor, and vRNP (10 ng of NP equivalents) in the presence or absence of purified proteins. RNA products were purified, subjected to 4% PAGE in the presence of 8 M urea, and visualized by autoradiography. For limited elongation assays, RNA synthesis was performed with vRNP (150 ng of NP equivalents) in the absence of UTP, and RNA products were separated by 15% PAGE containing 8 M urea. To address the encapsidation of nascent cRNA with NP, RNA synthesis was carried out by following the standard protocol described above except that 0.3 μM UTP, 250 μM each ATP, CTP, and GTP, and 10 μCi of [α-^{32}P]UTP (3,000 Ci/mmol) were used in a final volume of 200 μl. The coprecipitated RNA products with NP or MCM were separated through 10% PAGE containing 8 M urea.

Gene silencing mediated by siRNA. An siRNA against the RAF-2p48/UAP56 gene corresponding to its open reading frame (5′-AGUACUACGUGAAACU GAAGGACAA-3′) and control double-stranded RNA (dsRNA) targeting none of the cellular mRNAs were designed and synthesized by iGENE Therapeutics Inc. HeLa cells (1×10^5 cells) were transfected with 40 pmol of siRNA using Lipofectamine 2000 (Invitrogen) according to the manufacturer's protocol. At 48 h posttransfection, the cells were infected with influenza A/PR/8/34 at a multiplicity of infection (MOI) of 10 in the absence or presence of 100 μg/ml of cycloheximide (CHX). The RAF-2p48/UAP56 knockdown cells were also transfected with viral protein expression plasmids encoding PB1, PB2, PA, and NP and pHH21-vNS-Luc reporter plasmid to reconstitute a model viral replicon (19, 30). This reporter plasmid carries the luciferase (Luc) gene in reverse orientation sandwiched between 23-nucleotide (nt)-long 5′-terminal and 26-nucleotide-long 3′-terminal promoter sequences of the influenza virus segment 8, which is placed under the control of the human polymerase I (Pol I) promoter.

Indirect immunofluorescence assay. HeLa cells on coverslips were fixed with 4% paraformaldehyde in phosphate-buffered saline (PBS). The cells were permeabilized in 0.5% Triton X-100 and incubated in PBS containing 1% bovine serum albumin (BSA). The coverslips were incubated with anti-RAF-2p48/UAP56 rabbit polyclonal antibody (16) for 1 h. After a washing step with 0.1% Tween 20 in PBS, coverslips were incubated with Alexa Fluor 568-conjugated anti-rabbit IgG (Invitrogen) for 1 h. Images were acquired under the same exposure time by a fluorescence microscope system (Axiovision; Carl Zeiss).

Primer extension assay. Total RNAs isolated from control and RAF-2p48/UAP56 knockdown cells at 0, 3, 6, and 9 h postinfection (hpi) were subjected to reverse transcription at 42°C for 1 h with primers specific for segment 5 vRNA (5′-GGGAATACAGAGGGGAGAA-3′) corresponding to the NP cDNA between nucleotide sequence positions 1336 and 1354, segment 5 m/cRNA (5′-G ATTTCAGTGGCATTCTGGC-3′) complementary to the NP cDNA between nucleotide sequence positions 101 and 120, and 5S rRNA (5′-GGGGTACCTT CGAAAGCCTACAGCACCCGGTA-3′), which were labeled at their 5′ ends with [γ-^{32}P]ATP and T4 polynucleotide kinase (Toyobo). The products purified with phenol-chloroform extraction and ethanol precipitation were separated through 6% polyacrylamide gel containing 7 M urea and visualized by autoradiography.

Real-time quantitative PCR. Total RNAs isolated from control and RAF-2p48/UAP56 knockdown cells at 12 h posttransfection for construction of the model viral replicon were subjected to reverse transcription with primers to determine the level of vRNA (5′-TCCATCACGGTTTTGGAATGTTTACTA CAC-3′, which corresponds to the luciferase coding region between nucleotide sequence positions 728 and 757), cRNA (5′-AGTAGAAACAAGGGTGTTTT TTAGTA-3′, which is complementary to the 3′ portion of the segment 8 cRNA), and viral mRNA [oligo$(dT)_{20}$ for poly(A) tail] synthesized from the reconstituted model viral replicon. The synthesized single-stranded cDNAs were subjected to real-time quantitative PCR analysis (Thermal Cycler Dice Real Time System TP800; TaKaRa) with two specific primers, 5′-TCCATCACGGTTTTGGAAT GTTTACTACAC-3′, which corresponds to the luciferase coding region between nucleotide sequence positions 728 and 757, and 5′-GTGCGCCCCCAGAAGC AATTTC-3′, complementary to the luciferase coding region between nucleotide sequence positions 931 and 952. The amount of NP mRNA transcribed from the expression plasmid, which is transcribed by cellular RNA polymerase II, was detected as an internal control.

RESULTS AND DISCUSSION

Stimulation of *de novo* cRNA synthesis by NP. Exogenously added recombinant NP free of RNA (here, designated exogenous NP) stimulated *de novo* virus genome replication in the absence of MCM and any kind of primer (Fig. 1B, lanes 1 to 5). We confirmed by RNase H digestion analyses with primers corresponding to each segment that RNA products corresponded to those synthesized from each segment (data not shown). Then, we examined whether exogenous NP and MCM coordinately stimulate the virus genome replication reaction. MCM stimulated virus genome replication additively with recombinant NP, suggesting that NP and MCM function through distinct mechanisms (Fig. 1B, lanes 6 to 10 and 16 to 20). The stimulatory activity per molecule of MCM was five times higher than that of NP, as judged by the slopes of the lines in Fig. 1C (Fig. 1D). We observed that authentic NP free of RNA purified from virions by CsCl glycerol density gradient centrifugation (5, 34) stimulates activity equally as well as recombi-